

The transfer of energy between electrons and ions in solids

**A. P. Horsfield¹, D. R. Bowler^{1,2}, H. Ness³, C. G. Sánchez⁴,
T. N. Todorov⁵, and A. J. Fisher^{1,2}**

¹Department of Physics and Astronomy, University College London, Gower Street, London WC1E 6BT, United Kingdom

²London Centre for Nanotechnology, University College London, Gower St, London WC1E 6BT

³Service de Physique et de Chimie des Surfaces et Interfaces, DSM/DRECAM, CEA-Saclay, 91191 Gif sur Yvette, France

⁴Unidad de Matemática y Física, Facultad de Ciencias Químicas, INFQIC, Universidad Nacional de Córdoba, Ciudad Universitaria, 5000 Córdoba, Argentina

⁵School of Mathematics and Physics, Queen's University of Belfast, Belfast BT7 1NN, United Kingdom

E-mail: a.horsfield@ucl.ac.uk, david.bowler@ucl.ac.uk, t.todorov@qub.ac.uk, ness@dsm-mail.saclay.cea.fr

Abstract. In this review we consider those processes in condensed matter that involve the irreversible flow of energy between electrons and nuclei that follows from a system being taken out of equilibrium. We survey some of the more important experimental phenomena associated with these processes, followed by a number of theoretical techniques for studying them. The techniques considered are those that can be applied to systems containing many non-equivalent atoms. They include both perturbative approaches (Fermi's Golden Rule, and non-equilibrium Green's functions) and molecular dynamics based (the Ehrenfest approximation, surface hopping, semi-classical gaussian wavefunction methods and correlated electron-ion dynamics). These methods are described and characterised, with indications of their relative merits.

1. Introduction

This review is about the transfer of energy between electrons and nuclei. We focus especially on the theories and computer models that can be used to describe this process. Energy transfer is such a general concept, however, that we need to specify what exactly we have in mind here. A possible sequence of events that illustrates the kind of processes we have in mind is:

- (i) A system begins in equilibrium.
- (ii) It is then subjected to some external influence. This might be an electromagnetic pulse that transfers energy to the electrons thousands of times more efficiently than to the nuclei, thus giving the electrons a relatively higher energy. Or, at the other extreme, it might be a flux of neutrons which interact only with the nuclei which would have the effect of raising the energy of the nuclei relative to the electrons. (It could also be a number of other things, such as a beam of electrons or a flux of heat.)
- (iii) As a result of this departure from equilibrium, there will be a net flow of energy either from the electrons to the nuclei, or from the nuclei to the electrons, as the system moves back towards equilibrium.

The final transfer of energy is made possible by interactions that couple the electrons to the nuclei. Of course these same interactions lead to other forms of correlated motion between electrons and nuclei, such as the modification of the electronic band structure, the effective coupling between electrons that produces superconductivity, and the coherent transport of electrons by virtual polarons. Interesting though they are they are not covered here.

This review is structured as follows. In the next section we briefly summarise some relevant phenomenology. We then describe the most important methods currently available for modelling these phenomena. Finally we briefly consider the future of the theories.

2. Phenomenology

In this section we survey some phenomena observed in solids that are produced by the irreversible flow of energy between electrons and nuclei. In what follows, neither the range of phenomena nor the list of citations are exhaustive. Instead we have merely attempted to provide a basis for thought and analysis for the interested reader.

2.1. Joule heating

Probably the most familiar and easiest to observe phenomenon involving the inelastic transfer of energy between electrons and nuclei is the increase in temperature of an electrical conductor when a current passes through it. The idea that electric currents do work on conductors, and so cause heating, has been known since the mid nineteenth century when it was investigated by James Joule [1]. The treatment of transport in terms of Boltzmann's equation has been brought to a high level [2], with the coupling between the electrons and phonons treated perturbatively. This is accurate for macroscopic materials because no coupling to any one vibrational mode is large.

With the rise in interest in mesoscale and nanoscale systems additional quantum effects became apparent, introduced by the small length scales. One such system is the atomic scale contact, which can be produced either by a break junction or a scanning tunnelling microscope. When a current is passed through the junction heating takes place that increases with applied voltage. Experimental evidence for this heating comes from observations of the voltage dependence of two level fluctuations and hysteresis at conductance discontinuities in atomic scale contacts [3, 4] and from measurements on current induced rupture of atomic chains [5]. This heating, which can be very substantial, may at first seem mysterious since the electron mean free path is so much greater than an atomic spacing. However this net heating is simply a compromise between the small probability for an individual electron to scatter off a phonon in an atomic wire, and the huge density of current carrying electrons that accompanies the current densities attainable in quasi-ballistic metallic nanoconductors [6–8]. This can result in the apparent paradox of a hot conductor that is still largely ballistic, and thus resistance free, as far as individual electrons coming through are concerned.

2.2. Relaxation of excited electrons

The transfer of energy is not the only important consequence of the non-adiabatic interactions between electrons and nuclei. For example, non-radiative processes in semiconductors contribute to trapping of free carriers which has an impact on the conductivity and optical properties [9, 10]. Because the binding energy of deep centres can be much larger than typical phonon energies, the phonons can participate in the optical transitions (which provide the most direct information about the defect electronic properties). Thus non-radiative processes can be observed in optical absorption spectra of lattice defects [11].

Paramagnetic ions in insulators can undergo spin reversal [12] (the ions switch between Zeeman levels). Initially an electromagnetic field is applied. This takes the population away from equilibrium. The system can then return to equilibrium through interaction with thermal phonons [13], a process that can be observed by spin resonance experiments [14]. There is intense interest at present in similar phenomena in nanoscale systems such as quantum dots, as the quantum confinement produces discrete electronic states which modify the relaxation rates of electrons and holes [15–17].

Excitons can be thought of as a bound pair of particles: a negatively charged electron and a positively charged hole. Excitons can further interact with each other and form pairs [18], or bind to defects [19, 20]. However, since the hole is simply the absence of an electron, with the positive charge originating with the nuclei, it is possible for the two quasi-particles to combine and annihilate with the

release of energy. This energy can escape as a photon or one or more phonons. In semiconductors a phonon may be essential to the recombination process because of crystal momentum conservation, though the presence of defects that trap excitons can remove this constraint [19]. The angular momentum state of the exciton can frustrate its radiative decay [20], which is important for the efficiency of organic light-emitting diodes. A simple counting argument suggests roughly a quarter of excitons are in a singlet state (and can undergo radiative decay) while the remaining three quarters are in a triplet state (and cannot undergo radiative decay). However, there appear to be significant exceptions to this rule [21]. Excitons in quantum wells have increased binding energy because of their confinement, though their interaction with phonons appears unaffected [22]. In multiple quantum well structures, excitons can become trapped at a number of sites with different energies. Phonons assist in the migration at low temperatures (making up the difference in energies between binding sites), and at higher temperatures ($>10\text{K}$) produce thermally activated migration [23].

2.3. Inelastic electron tunnelling spectroscopy

Inelastic electron tunnelling spectroscopy exploits the transfer of energy between electrons and nuclei to probe the vibrational spectrum of molecules by passing an electric current through them. A schematic of the experimental arrangement is shown in figure 1. There are two metallic plates (or contacts) across which a bias is applied ($eV = \mu_L - \mu_R$, where V is the applied voltage and μ_L and μ_R are the chemical potentials of the left and right plates respectively, as shown in figure 1). Between the plates is an insulating region (often an oxide) that contains the molecules whose vibrational frequencies we wish to probe. In general there will be an elastic tunnelling current (an electron arrives at the right plate with the same energy that it had when it departed the left plate) whose magnitude increases linearly with the applied voltage for low voltages. At low temperatures, and for sufficiently large applied voltage ($eV \geq \hbar\omega_0$ where ω_0 is the angular frequency for the vibrational mode with lowest frequency that can exchange energy with an electron), a conduction channel will open up in which an electron can arrive at the right hand plate and enter an empty state with a diminished energy, the energy lost being equal to one quantum of vibrational energy for the molecules in the sample. By increasing the voltage, additional channels open up corresponding to higher vibrational frequencies, or possibly multi-phonon processes. At higher temperatures it is possible for the electron to gain energy from the molecular oscillations.

Lambe and Jaklevic [24] present a theory based on Fermi's Golden Rule (see section 3.2.2) suitable for oxides in which the electron exchanges energy remotely from the oscillators through an electrostatic dipole interaction. They also report experimental results for a system consisting of Al and Pb plates sandwiching Al_2O_3 doped with small organic molecules. The experiments were performed from below 1K up to 300K, and inelastic resonances corresponding to molecular vibrational frequencies were detected as peaks in the second derivative of the current-voltage curve (d^2I/dV^2). Klein *et al* [25] used a similar technique, and found that different ranges of voltage probed not only the frequencies of the impurities but also of the contacts and the oxide. The technique for absorbing molecules was improved by Simonsen *et al* [26] who used the liquid phase of the molecules. This made it possible for them to investigate the vibrational frequency spectrum of much larger molecules including proteins and nucleotides. Kirtley and co-workers have made a series of

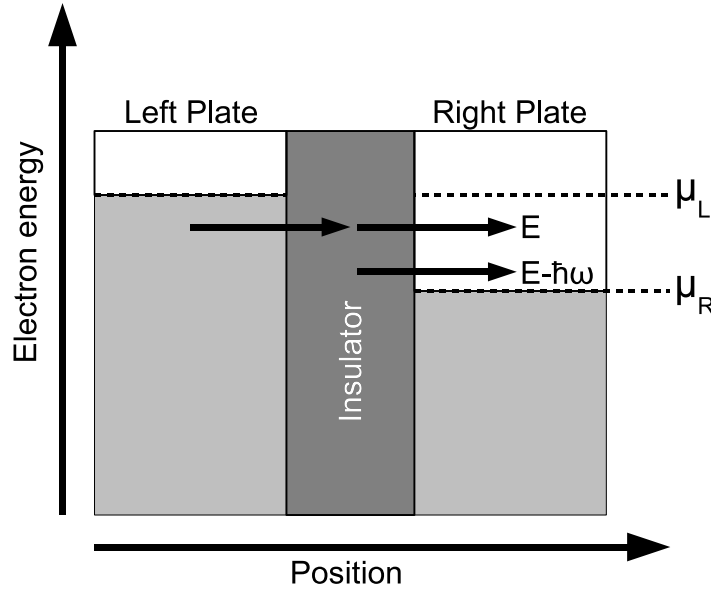


Figure 1. The arrangement for inelastic electron tunneling spectroscopy. There are two metallic plates, between which is an insulating layer. A voltage is applied, so the electron chemical potentials of the two plates become offset, allowing electrons to flow from filled states on the left to empty states on the right. In the insulating sample there are molecules that can exchange energy with a tunneling electron: the electron can excite a vibration of angular frequency ω in the molecule, and so lose energy $\hbar\omega$.

contributions [27–31]. They have investigated the effect of the choices of metal and oxide for the tunnelling device, and found that these can influence the measured spectra [27, 29]. They have developed a theory of the intensities of the vibrational modes using a transfer-Hamiltonian formalism with WKB wavefunctions [28]. In this model the interaction between the tunnelling electron and an oscillating molecule is through the Coulomb interaction with the partial charges on the molecule. It has been applied to CH_3SO_3^- chemisorbed on alumina [31]. Multiple scattering $\text{X}\alpha$ calculations showed that this long ranged potential indeed dominates the measured spectra [30].

Persson and Baratoff [32] showed that the excitation and immediate de-excitation of a molecular vibration by a tunnelling electron can give a decrease in the resonant conductance. A closely related problem is the inelastic current voltage spectroscopy of a ballistic atomic metallic chain [33, 34], or a single resonant molecule between two electrodes [35]. The opening of new inelastic scattering channels, as the bias matches the energies of various phonon modes in the wire, also leads to a suppression of the electronic conductance, since, starting from ideal transmission, the conductance can only ever go down, and the inelastic I-V features take the form of dips in d^2I/dV^2 .

Scanning tunnelling microscopes (STMs) have been used for inelastic spectroscopy. Inspired by this, Gregory [36] created a very small junction by using two crossing gold wires with argon and carbon monoxide in between. Resonant peaks were observed from hydrocarbon contaminants, as was Coulomb blockade behaviour. Ho and co-workers [37–40] have used an STM to probe the orientation, motion and

vibrational spectra of small molecules on metal surfaces. Yu *et al.* studied a molecular transistor and found shifts in the resonances when the gate voltage was varied. With the experimental advances has gone developments in the theory. Lorente and Persson [41] used density functional theory and a perturbative implementation of non-equilibrium Green's functions (NEGF) to study C₂H₂ and C₂HD on Cu(100), and Galperin *et al.* [42] used NEGF and a model Hamiltonian to study line shapes and line widths of IETS features.

2.4. Friction force on high energy particles

The bombardment of materials by high energy heavy particles occurs in a number of situations. Ions with energies of order 10 keV are used for ion implantation in semiconductors [43], while in hydrogen fusion powerplants materials of quite extraordinary resilience are required to surround the region containing the plasma because they are subjected to bombardment by highly energetic neutrons (14.1 MeV) and other particles as well as exposure to very high temperatures [44].

Ion implantation of semiconductors is well understood [11, 43]. The type of scattering experienced by the implanted ion depends on the mass of the ion and the relative angle of its trajectory to the crystallographic axis. The distribution of implanted ions is a gaussian centred about the projected range. The projected range in turn is determined by the stopping power which has contributions both from the nuclei in the crystal and from the electrons. The stopping power (S) is defined by the projected range (R_p) through $R_p = \int_0^{E_c} dE/S(E)$, and is a sum of the nuclear and electronic components ($S = S_n + S_e$). The electronic component has a very simple form, namely $S_e(E) = k_e \sqrt{E}$, where k_e is a constant (in silicon it has the value $10^7 \sqrt{\text{eV}/\text{cm}}$). As the stopping power has the dimensions of a force, and is proportional to the velocity of the incoming ion ($v = \sqrt{2E/M}$), it is behaving as a kind of friction.

There has been considerable interest in the properties of candidate materials for fusion powerplants under extreme conditions, and extensive modelling work has been performed [45]. Clearly the collisions between atoms to form cascades is an extremely important process, but the dynamics of the atoms is significantly modified by the response of the electrons to this violent motion. The dynamics of radiation damage is typically divided into three phases: the displacement phase, the relaxation phase and the cooling phase. The details of the interaction between the nuclei and electrons need not be the same in each phase because of the large variation in the energy of both the nuclei and the electrons between the phases. Further, the manner in which electrons transport heat is also modified when they become highly excited [46], or the lattice highly disordered [47]. There is still some controversy about precisely what happens, but there are some general ideas which are clear. Highly energetic nuclei can give up substantial amounts of energy to the electrons [48], and in so doing experience an effective friction force [49]. As the coefficient of friction depends on materials parameters such as electron-phonon coupling strength and electron heat capacity, it leads to different rates of cooling in different materials, which in turn can modify both defect formation and healing of damage [49].

There is a rather different type of process in which electrons (light particles) are used to bombard a metal to produce damage (displacement of heavy particles) though at quite a low level (2×10^{-6} to 2×10^{-4} displacements per atom). Subsequent measurement of the variation of resistance as a function of increasing temperature during annealing of the damaged material provides direct information about the

diffusion barrier heights of point defects, which would be difficult to obtain any other way [50].

3. Theoretical methods and their applications

As all theories involve some kind of simplification of reality, they must all throw away features that are considered unimportant. However, there will always be cases where what is normally unimportant suddenly takes centre stage. When thinking about the interaction of atoms with each other, it is usually a very good approximation to assume that the electrons are so light, and thus move so fast relative to the nuclei, that over the time it takes for the nuclei to undergo a significant displacement (say 10^{-13} s), the electrons will have undergone so many collisions, both with nuclei (possibly as much as 1000 times in a simple classical view) and with each other, that they will have settled down into a well-defined state (normally taken to be their ground state, or more generally that state which minimizes the chosen free energy). Thus, we can treat the state of the electrons as known once the *positions* of the nuclei are given. This is the Born-Oppenheimer approximation, whose chief characteristic is that it allows us to treat the electrons and ions separately, and is ubiquitous because it greatly simplifies the process of understanding matter at the atomic scale.

However, the Born-Oppenheimer separation is an approximation, and there are phenomena it cannot describe, notably those that are the subject of this review. To understand the nature of this approximation, and why it is unable to describe the irreversible transfer of energy between electrons and nuclei, we need only note the following. Even if the nuclei start at rest, collisions with electrons will result in small energy transfers to nuclei (of order 0.1% or less of the electron energy per collision, classically). Once they have started to fluctuate, the nuclei can transfer kinetic energy back to the electrons in individual electron-nuclear collisions. But this two-way inelastic energy transfer depends on the *velocities* of the colliding particles. This dependence lies beyond the Born-Oppenheimer approximation.

Fortunately, the amount of energy transferred in one collision is very small. Thus the departure from the Born-Oppenheimer approximation is a rather weak effect and so it makes sense to use perturbation theory. The perturbation can be characterised by those contributions to the forces on the nuclei that involve *two* electronic states, corresponding to electrons scattering from one state to another. The unperturbed electronic states are some representation of the Born-Oppenheimer energy surfaces, and for the nuclei harmonic oscillator states associated with small displacements from equilibrium positions on those surfaces are usually used (see Appendix A). Lowest order perturbation theory can then be used to evaluate the rate of change of some quantity (such as the degree of excitation of the nuclear vibrations) as a result of the perturbation. For systems in which well-defined reference states can be defined, this prescription provides not only insight into mechanisms, but also numbers that can be compared with experiment. Examples include Joule heating in metals and non-radiative transitions at point defects in semiconductors.

However, there are systems in which it is difficult to set up the reference systems. If the nuclei undergo substantial displacements, so that the concept of a reference position is not well-defined (for example, flexible polymer strands in contact with a heat bath, or a metal subject to high-energy bombardment) then neither the electronic nor nuclear states are straightforward to characterise. However, such systems have the feature that much of their behaviour can be well described by molecular dynamics

carried out within the Born-Oppenheimer approximation. So, the natural consequence is to see if the standard molecular dynamics algorithms can be revised to include the effects of the breakdown of the Born-Oppenheimer approximation. Since the full coupled problem is insoluble except in the simplest of cases we have to investigate possible approximations.

In the following sections we discuss possible mathematical methods, both perturbative and molecular dynamics based, that can be used to investigate non-adiabatic processes. We begin with a simple classical model in which both the nuclei and the electrons are treated as classical particles obeying Newton's equations of motion. This cannot be considered a particularly realistic model, but it is simple to understand and in fact reveals much of the physics. We then proceed with the methods that make explicit use of Born-Oppenheimer surfaces and oscillator states, both perturbative and non-perturbative. Finally we survey the methods based on molecular dynamics.

3.1. Classical model

While a classical model of the motion of electrons may not provide us with a quantitative scheme in general, it makes it easy to understand inelastic processes. To illustrate the points made we will look at the heating of an atom by a current of electrons [51].

The physical setup is as follows. We have an atom in a solid for which the influence of the neighbouring atoms is represented by a spring (an Einstein model). The electrons we treat as independent particles which can interact with the oscillating atom. The Hamiltonian for the system is the sum of an electron Hamiltonian (H_e), an atom Hamiltonian (H_A) and a coupling Hamiltonian (H_{eA})

$$H = \underbrace{\sum_i \left(\frac{p_i^2}{2m} + v(\vec{r}_i) \right)}_{H_e} + \underbrace{\left(\frac{P^2}{2M} + \frac{1}{2} K X^2 \right)}_{H_A} - \underbrace{\sum_i \vec{X} \cdot \vec{\nabla} v(\vec{r}_i)}_{H_{eA}} \quad (1)$$

where $v(\vec{r}_i - \vec{X})$ is the interaction potential between electron i and the atom, and we have made the approximation $v(\vec{r}_i - \vec{X}) \approx v(\vec{r}_i) - \sum_i \vec{X} \cdot \vec{\nabla} v(\vec{r}_i)$, which corresponds to small atomic displacements. Using Hamilton's equations we can write down the equations of motion for the electrons and for the atom

$$\begin{aligned} M \ddot{X}_\nu &= -K X_\nu + \sum_i \frac{\partial v(\vec{r}_i)}{\partial r_{i\nu}} \\ m \ddot{r}_{i\nu} &= -\frac{\partial v(\vec{r}_i)}{\partial r_{i\nu}} + \sum_{\nu'} X_{\nu'} \frac{\partial^2 v(\vec{r}_i)}{\partial r_{i\nu'} \partial r_{i\nu}} \end{aligned} \quad (2)$$

In the absence of the coupling Hamiltonian H_{eA} , from Eq. 2 we can write down an explicit solution for the atomic motion ($X_\nu(t) = A_\nu \sin(\sqrt{K/M}t + \phi_\nu)$). Furthermore, the electrons move independently of one another, with each electron moving with a constant energy (the scattering from the atom is elastic). Once we include the coupling Hamiltonian, this all changes. We can no longer write down a simple closed form expression for the atomic motion as it now depends on all the electrons; the electrons are no longer completely independent because their motion depends on \vec{X} , which in turn depends on all the electrons; and electrons no longer move with constant

energy because they experience an external time varying force. It is the third point that is the main topic of this review.

We can solve these equations for the case of motion in one dimension in which the atom appears as a hard wall potential to the electrons. In this case, by conserving energy and momentum during a collision, we get the following approximate expression [51] for the power delivered to the atom (w) by a current (j) of electrons in the limit that the electrons are much lighter than the atom

$$w \approx 4j \left(\frac{m}{M} \right) (K_e - 2K_A) \quad (3)$$

where K_e and K_A are the mean kinetic energies for the electrons and atom respectively. We see that there are two contributions, one positive from the electrons (which provides heating) and one negative from the atom (which leads to cooling). The energy scale relevant to the electron kinetic energy is eV , where V is the applied bias. At low temperatures, the energy scale relevant to the atom kinetic energy is $\hbar\omega$ where ω is the vibrational frequency of the atom. Thus for very small bias we might expect cooling, but for typical voltages we expect the electrons to heat the atom, as is indeed observed.

Equations 2 enable us also to see explicitly the microscopic correlated electron-nuclear fluctuations that nucleate non-radiative inelastic processes and mediate the inelastic exchange of energy between the two subsystems. Consider an electron bound in an orbit with radius r and speed v around a nucleus. The nucleus starts off at rest, at the bottom of the parabolic well provided by the rest of the lattice. Let us solve Eq. 2 approximately as follows. To lowest order, ignore the motion of X in the second equation. Then the electron remains in the original orbit and provides a sinusoidally varying external force on the nucleus, of amplitude $F = mv^2/r$ and frequency $\omega = v/r$, along each of the two axes in whose plane the orbit lies. The nucleus in turn is now a driven harmonic oscillator. If we solve the equation motion for the nucleus assuming that it starts at rest, then the average kinetic energy over one period of oscillation of the nucleus is given by

$$K_A = \frac{1}{2} \frac{F^2}{M} \frac{1}{2} \frac{3\omega^2 + \omega_0^2}{(\omega^2 - \omega_0^2)^2}$$

If $\omega \rightarrow \omega_0$, we see a resonance, with violent heating of the nucleus. This resonance is the classical analogue of the quantum transitions that become activated when the two frequencies match. In the limit $\omega \gg \omega_0$, on the other hand, K_A settles at

$$K_A = \frac{3}{2} \frac{m}{M} K_e$$

where $K_e = mv^2/2$. The nucleus has acquired some kinetic energy, and thus is no longer sitting still. The underlying motion of the nucleus, responsible for K_A above, is the wobble of a heavy particle induced by the passage of a light particle, familiar from planetary physics. As a consequence of this correlated wobble, nuclei are never truly frozen: momentum conservation, with the consequence that light and heavy particles always orbit a common centre of mass, leads to a repartitioning of energy between the two systems, in a ratio controlled by m/M .

3.2. Born-Oppenheimer based electron-phonon coupling formalism

In this section we consider those methods that make explicit use of energy surfaces, and the non-adiabatic coupling between them.

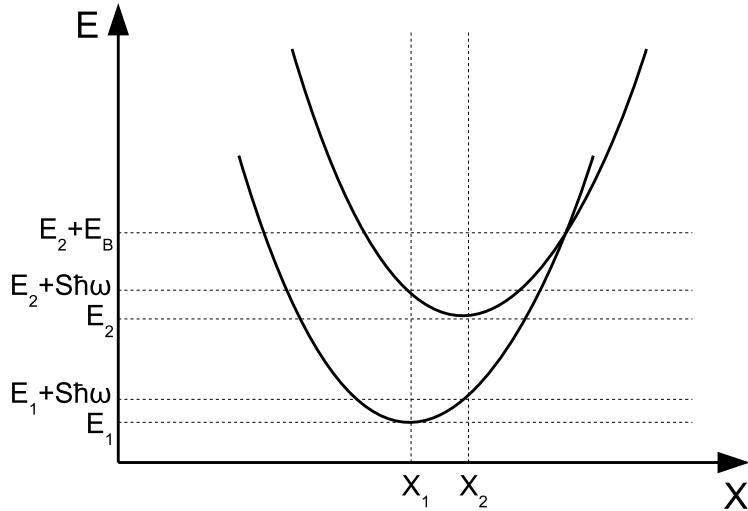


Figure 2. The parameters characterising a two level system. The Landau-Zener theory concentrates on the crossing region on the right-hand side of the diagram.

3.2.1. Landau-Zener theory There is a generic model that has been successfully applied to a huge number of problems: it is the two level harmonic model (or spin-boson Hamiltonian) and is often considered in the presence of a dissipative bath [52]. It has the advantage of providing useful insights pictorially as well as through numbers. In figure 2 is shown a representative system. The two diabatic surfaces (see Appendix A) have the same curvature (vibrational frequency), but their minima are offset relative to each other both in energy and position. There are three other characteristic energies, two associated with vertical (for example, optical) transitions ($E_1 + S\hbar\omega$ and $E_2 + S\hbar\omega$, where S is the Huang-Rhys factor), and one associated with non-radiative transitions ($E_2 + E_B$). It is the latter that interests us here.

The quantity E_B is the barrier height that a classical oscillator on the upper energy surface has to overcome to cross onto the lower energy surface. The transition between the surfaces is a quantum process (involving an electronic transition). This can correspond to a number of physical phenomena, with an important one in the solid state being electron capture (or emission) by a charge trap in a semiconductor [53], and another being atomic collisions with crystal surfaces [54]. This combination of quantum and classical descriptions was turned into a transition rate in 1932 both by Zener and Landau [55, 56], and has been extended in a number of ways since (see for example [57, 58]).

The essence of the original Landau-Zener theory is as follows. The oscillating atoms (represented by just one coordinate, X in figure 2, and from now on referred to as the oscillator) move on a diabatic energy surface. The coupling to the neighbouring surface is so weak (because of charge rearrangement in the case Zener studied) that a transition is unlikely, so we can neglect the influence of the transition on the dynamics of the oscillator for the purpose of determining the transition rate. No transition is possible except very near to the crossing. In this region the energy surfaces are treated

as linear, and the velocity of the oscillator as constant. By solving the time dependent Schrödinger equation for the electrons subject to the time varying potential due to the oscillator, the probability of a transition during one pass of the oscillator over the crossing is found to be [55] $P_X = \exp(-2\pi\gamma)$ with

$$\gamma = \frac{|E_{12}|^2}{\hbar} \left(\frac{d(E_1 - E_2)}{dt} \right)^{-1} \quad (4)$$

where E_{12} is the electronic matrix element coupling the two surfaces, and $E_1 - E_2$ is the energy difference between the surfaces. The transition rate is then given by $\Gamma = 2fP_X$ [59] where f is the vibrational frequency.

3.2.2. Perturbation theory There is a long history of using perturbation theory for studying non-adiabatic processes, both in the solid state and elsewhere. A very important context for its use is in the Boltzmann equation treatment of the transport properties of solids [2]. Fermi's Golden Rule gives the transition rate from state $|i\rangle$ to state $|f\rangle$

$$\Gamma_{i \rightarrow f} = \frac{2\pi}{\hbar} \left| \langle f | \hat{H}_1 | i \rangle \right|^2 \delta(E_f - E_i) \quad (5)$$

where $E_i = \langle i | \hat{H}_0 | i \rangle$ and $E_f = \langle f | \hat{H}_0 | f \rangle$, \hat{H}_0 is the unperturbed Hamiltonian, and \hat{H}_1 is the perturbing Hamiltonian driving the transition. For the case of interest to us (electrons interacting with mobile nuclei) from Appendix A we can identify $|i\rangle$ with $|\Psi_{nN}\rangle$, $|f\rangle$ with $|\Psi_{n'N'}\rangle$, E_i with U_{nN} and E_f with $U_{n'N'}$, where n indexes electronic states and N indexes nuclear states. To make the integrals in the energies and transition matrix elements tractable, the harmonic approximation is used for the nuclear states. For the adiabatic representation (see Appendix A) some further decisions about the dependence of the electronic wave functions on nuclear coordinate is also necessary. These decisions are implicit in the static lattice representation. In the context of non-radiative transitions the choice of approximation is discussed in detail by Stoneham in review articles [9, 60] and a book [10]. Once the rates are known, experimentally observable quantities can be determined such as vibrational lifetimes of adsorbed molecules [61], or the power supplied to atoms (w) during electric current induced heating in nanocontacts [8, 62]. The power is given by

$$w = \frac{2\pi}{\hbar} \sum_{n'N'} |\langle \Psi_{n'N'} | \hat{H}_1 | \Psi_{nN} \rangle|^2 (W_{N'} - W_N) \delta(U_{n'N'} - U_{nN}) \quad (6)$$

where W_N is the energy of the nuclei in state N . These matrix elements have been calculated, within tight binding and density functional theory, for atomic and molecular wires [62–68]. The power into a phonon mode has the structure

$$w = \frac{\pi\hbar}{M} \sum_{\alpha\beta} f_\alpha (1 - f_\beta) |\langle \beta | \vec{g} | \alpha \rangle|^2 \{ (N + 1) \delta[\epsilon_\alpha - (\epsilon_\beta + \hbar\omega)] - N \delta[\epsilon_\alpha - (\epsilon_\beta - \hbar\omega)] \} \quad (7)$$

where $|\alpha\rangle$ is a single particle electronic orbital with eigenvalue ϵ_α and occupancy f_α , and \vec{g} is the gradient of the electronic Hamiltonian with respect to the oscillator normal coordinate. The phonon frequency is ω and its occupancy is N . For simplicity we have assumed that all comic masses are the same, M , but in practice this assumption is easily lifted. Equation 7 accounts for the observed heating in nanocontacts [8, 62, 65]. The same perturbative model can also account for some of the inelastic current-voltage features in atomic and molecular wires [63, 66–68].

Lowest order perturbation theory clearly cannot handle multiple coherent transitions or strong interactions [69]. However, higher order theories can be used in these cases (see 3.2.3). Problems where higher order theories have been used include the non-adiabatic transition at a crossing between two electronic levels in the presence of dissipation [58], cross-sections for inelastic scattering of electrons from a surface [70] and inelastic tunneling cross-sections [71].

3.2.3. Non-equilibrium Green's functions Green's functions are one of the well established tools for dealing with problems in condensed matter. They provide information about the response at any point in space-time due to an excitation (usually the creation or annihilation of a particle) at any other point. Green's functions are used in perturbation theory, linear response theory, and quantum kinetic equations. Their real power becomes evident when we consider a system of many particles (electrons and nuclei) that interact, and more especially when the system is being driven out of equilibrium by some external forces. Their application to transport, in the framework of the Keldysh formalism, has a long history [72–78]. In the absence of particle interactions, the many-body Keldysh formalism reduces [79] to the steady-state transport formalism based on one-electron Lippmann-Schwinger scattering theory (for a brief review see [80]), which in turn reduces [78] to the Landauer formalism. In the following, we present some applications of the Green's functions technique for systems with interactions between electrons and atomic motion. Note that in this section (and the corresponding appendices) we depart from the usual notation for representing all operators by means of hats (such as \hat{H}_e) to avoid a confusion of extra symbols. Instead hats are used to represent only operators in the interaction picture.

Beyond perturbation theory: Let us start by generalizing Fermi's golden rule to include higher-order terms in the perturbation V . The formal derivation based on scattering theory is rather involved, therefore we consider a simpler approach following the prescription given in Refs. [81–83]. This will permit us to introduce the different quantities that are needed in the full description based on non-equilibrium statistical physics [84, 85].

Let us assume that the perturbation V in the full Hamiltonian $H = H_0 + V$ is turned on adiabatically in the distant past, *i.e.* $V \equiv V e^{\eta t/\hbar}$ (with η a small positive constant). Initially the system is, at time t_0 , in the state $|i\rangle$ and evolves at time $t > t_0$ into the state $|i(t)\rangle$:

$$|i(t)\rangle = e^{-iH_0 t/\hbar} \hat{U}(t, t_0) e^{iH_0 t_0/\hbar} |i\rangle, \quad (8)$$

where $\hat{U}(t, t_0)$ is the time evolution operator (given within the interaction picture) of the system. The probability $P(t)$ to find the system in the final state $|f\rangle$ at time t is given by $|\langle f | i(t) \rangle|^2$ and its time derivative gives the transition rate $\Gamma_{fi} = \Gamma_{i \rightarrow f}$. To derive the generalized Fermi's golden rule, we include all orders of the perturbation V in the time evolution operator \hat{U} . Then, we have

$$\langle f | i(t) \rangle = \langle f | \hat{U}(t, t_0) | i \rangle e^{-iE_f t/\hbar} e^{iE_i t_0/\hbar}, \quad (9)$$

with

$$\begin{aligned} \hat{U}(t, t_0) &= \sum_n \frac{1}{(i\hbar)^n} \int_{t_0}^t dt_1 \int_{t_0}^{t_1} dt_2 \int_{t_0}^{t_2} dt_3 \dots \int_{t_0}^{t_{n-1}} dt_n \hat{V}(t_1) \hat{V}(t_2) \dots \hat{V}(t_n) e^{\eta t_n/\hbar} \\ &= \sum_{n=0}^{\infty} \frac{1}{n!} \frac{1}{(i\hbar)^n} \int_{t_0}^t dt_1 \dots \int_{t_0}^t dt_n T_t \left(\hat{V}(t_1) \dots \hat{V}(t_n) \right) = T_t \left(\exp \left(-\frac{i}{\hbar} \int_{t_0}^t d\tau \hat{V}(\tau) \right) \right) \mathbb{1} \end{aligned}$$

where the perturbation $\hat{V}(t)$ is taken in the interaction representation $\hat{V}(t) = e^{iH_0 t/\hbar} V e^{-iH_0 t/\hbar}$ and T_t denotes the time ordering operator. Performing the time integrations and making use of the interaction picture for the perturbation, we obtain

$$P(t) = |\langle f | i(t) \rangle|^2 = \left| \frac{e^{\eta t/\hbar}}{E_i - E_f + i\eta} \langle f | T | i \rangle \right|^2, \quad (11)$$

and identifying the time derivative of $P(t)$ with the transition rate Γ_{fi} , one finds the generalised Fermi's golden rule:

$$\Gamma_{fi} = \frac{2\pi}{\hbar} |\langle f | T | i \rangle|^2 \delta(E_f - E_i). \quad (12)$$

The quantity T in Eq. (11) is called the T -matrix and is given by the series expansion

$$T = V + V \frac{1}{E_i - H_0 + i\eta} V + V \frac{1}{E_i - H_0 + i\eta} V \frac{1}{E_i - H_0 + i\eta} V + \dots \quad (13)$$

For the lowest-order expansion $T \approx V$ or equivalently by taking $\hat{U}(t, t_0) \approx 1 - i/\hbar \int_{t_0}^t dt' \hat{V}(t')$ in Eq. (10), one recovers the transition rate $\Gamma_{fi} = \Gamma_{i \rightarrow f}$ given by the usual Fermi's golden rule Eq. 5.

The T -matrix can be rewritten in a compact and closed form

$$T = V + V \frac{1}{E_i - H_0 + i\eta} T = V + V G_0^r T \quad (14)$$

which generates the same series as in Eq. 13. This allows us to introduce one of the different Green's functions, namely the retarded Green's function G_0^r defined, in the energy representation, by $G_0^r(\omega) = [\omega - H_0 + i\eta]^{-1}$. This Green's function is obtained from the unperturbed Hamiltonian H_0 . The retarded Green's function G^r for the total Hamiltonian $H = H_0 + V$ is defined by $G^r(\omega) = [\omega - H + i\eta]^{-1}$. Then, the T -matrix can be expressed as $T = V + V G_0^r T = V + V G V$ by making use of the Dyson equation that links the full Green's function to the unperturbed Green's function: $G^r = G_0^r + G_0^r V G^r = G_0^r + G_0^r T G_0^r$. Now we have all the ingredients to develop the non-equilibrium theory, namely the concept of Green's functions, the time evolution operator and the Dyson equation. One already sees the importance of using Green's functions in determining transition rates when going beyond perturbation theory. Obviously, the conventional results of perturbation theory are obtained by expanding the Green's function in the Dyson equation or the T -matrix to the lowest-order in the perturbation.

The T -matrix formalism with scattering boundary conditions has been used to study the effects of electron-atomic vibration coupling in the transport properties of atomic and molecular wires. This was done (i) to the lowest-order in the interaction, *i.e.* perturbation theory, in atomic wires [62–64] and molecular wires [65–67]; and (ii) to all orders in the interaction in model systems and molecular wires by using conventional Green's functions techniques [86–97]. The connection between the inelastic T -matrix scattering formalism and non-equilibrium Green's functions has been discussed in Ref. [98].

Interaction as self-energy in the Green's functions: To describe the ground state or the thermal-averaged properties of a system of many particles, such as the coupled electron/atom system considered in this paper, it is useful to work with a many-body approach based on Green's functions. Such a Green's functions approach is even more useful and powerful when we want to calculate the properties of the system driven out

of equilibrium by some external forces. The exact definitions of the different Green's functions and their interrelation is given in Appendix C as well as the principles used to derive the theory for non-equilibrium conditions.

Now, it is important to define precisely what the perturbation V means physically. Here we consider V as being a perturbation on the reference system (described by the unperturbed Hamiltonian H_0) due to some kind of interaction. It is convenient to distinguish between different kinds of interaction, though generally speaking the calculation of such interactions and their inclusion in the Green's functions are formally equivalent for all kinds of interactions. In the following, it is convenient to consider as separate the following interactions:

- (i) The interactions between particles, *i.e.* the interactions between electrons, between phonons, or the interaction between electrons and phonons (or atomic motion). In practice, such interactions are incorporated in the corresponding electron or phonon Green's functions under the form of a proper self-energy via a Dyson-like equation for the Green's function. In the literature, it is usual to talk about electron Green's functions being dressed by the phonons, and phonon Green's functions being dressed by the electrons. The corresponding self-energies are usually difficult to calculate exactly for a many-particle system. They are obtained, up to some order in the interaction parameters, via the use of a many-body Feynman diagrammatic perturbation theory [99, 100].
- (ii) The interactions of the particles with an external field. As an example, one can consider an electromagnetic field exciting the electronic system by inducing electronic transitions, or an external applied bias that drives a nanojunction out of equilibrium by establishing a steady-state current flow. The corresponding hot electrons would then transfer energy to the phonon degrees of freedom via some interaction of type (i) mentioned above.
- (iii) It is often interesting to partition a system into its different constituent parts. For example: a crystal partitioned into a localized region around a defect and the rest of the crystal; a surface with adsorbate partitioned into the bare surface and the adsorbate; a nano-junction partitioned into three parts (a central region whose transport properties are studied and the two electrodes to which the central region is connected). In this case, the interaction between two different parts (I) and (II) of the system (for example the part of the electronic Hamiltonian that couples regions (I) and (II)) appears under the form of a self-energy in the Green's functions expanded onto the subspace of one of these regions. Often these self-energies are also referred to as embedding potentials [101]. These self-energies are usually practical to calculate, especially for systems treated within a mean-field approach and when there is no crossing of the interactions of type (i) between regions (I) and (II).

We now consider that the system has either reached a stationary-state regime or more simply is at equilibrium. Then the Green's functions depend only on the time difference $t - t'$, and their Fourier-transform $G^x(\omega)$ depend on only one energy argument ω . In the presence of interactions, the electron Green's function $G^{r,a}$ obeys a Dyson equation (either at equilibrium or in a non-equilibrium regime): $G^{r,a}(\omega) = G_0^{r,a}(\omega) + G_0^{r,a}(\omega)\Sigma^{r,a}(\omega)G^{r,a}(\omega)$ where $G_0^{r,a}$ is the Green's function of the electronic system in the absence of the interactions, and $\Sigma^{r,a}$ is the self-energy arising from these interactions. A similar Dyson equation relates the phonon Green's

function $D^{r,a}$ in the presence of interactions to the undressed phonon Green's function $D_0^{r,a}$ (see Appendix C). For the non-equilibrium state, the Green's functions $G^{<,>}$ and $D^{<,>}$ obey another kind of quantum kinetic equation (see below or Appendix C).

The difficulty is to calculate exactly, or as accurately as possible, the different Green's functions by including all orders of the different kinds of interactions. It is also a challenge to calculate them numerically because the self-energies $\Sigma^{x=(r,a,<,>)}$ arising from the interactions are actually functionals of the different Green's functions themselves: $\Sigma^x(\omega) = \Sigma^x[\{G^x(\omega)\}, \{G_0^x(\omega)\}]$ where G^x (G_0^x) denotes a Green's function in the presence (absence) of the interactions respectively.

One way of solving the problem approximately is to expand the Dyson equation in a Born series of the Green's function G_0 in the absence of the interactions, $G = G_0 + G_0 \Sigma G_0 + G_0 \Sigma G_0 \Sigma G_0 \Sigma G_0 + \dots$, then choose lower-order Feynman diagrams in the interaction parameters for the proper self-energy Σ (the Born approximation), and finally substitute the Green's function G_0 in the expression of the self-energy by the full Green's function G . In this way, one introduces a self-consistent scheme since the Green's function G both determines and is determined by the proper self-energy Σ . This approximation is usually known as the self-consistent Born approximation (SCBA). Physically it means that the interaction is treated to all orders but that only a limited number of elementary excitations are generated, *i.e.* those given by the many-body diagrams chosen for the self-energy. Within the SCBA some processes involving crossed diagrams are omitted (if they were not already included in the self-energy).

Now that we have described the principle of non-equilibrium Green's functions and the ways to include the interactions, we consider an example of their use in relation to electronic transport through a heterojunction in the presence of an electron-phonon interaction. Then we will briefly describe how they can be used to derive quantum kinetic equations as a generalisation of the Boltzmann equation for transport.

Electronic current in the presence of interaction: Let us consider a scattering central region (a quantum dot, a molecular or atomic wire) in which there are interactions between particles, and which is connected to two (left L and right R) leads. The latter are described by two non-interacting Fermi seas at their own equilibrium and thus characterised by two Fermi distributions f_L and f_R . The electronic current J_L flowing from the left lead into the central region is then expressed in terms of three Green's functions ($G^{r,a}$ and $G^<$) of the interacting central region. In the stationary-state regime, the current J_L is given by [72, 73, 75, 78, 102]:

$$J_L = \frac{ie}{h} \int d\omega \text{Tr} \{ f_L(\omega) \Gamma_L(\omega) [G^r(\omega) - G^a(\omega)] + \Gamma_L(\omega) G^<(\omega) \} , \quad (15)$$

where the trace runs over the electron states of the central region and Γ_L is related to the imaginary part of the retarded (advanced) self-energy $\Sigma_L^{r(a)}$ arising from the coupling of the central region to the left lead (self-energy arising from an interaction of type (iii) — see above). These self-energies and other self-energies arising from the other kinds of interactions should be included in the calculation of $G^{r(a)}$.

An expression similar to Eq. 15 can be obtained for the current J_R flowing from the right lead into the central region by interchanging the subscript $L \leftrightarrow R$ in Eq. 15. For a current conserving system, one has $J_L = -J_R$. The famous result of Meir and

Wingreen [78] is obtained from the symmetrised current $J = \frac{1}{2}(J_L - J_R)$

$$J = \frac{ie}{2h} \int d\omega \text{Tr} \{ (f_L(\omega) \Gamma_L(\omega) - f_R(\omega) \Gamma_R(\omega)) [G^r(\omega) - G^a(\omega)] + (\Gamma_L(\omega) - \Gamma_R(\omega)) G^<(\omega) \} \quad (16)$$

By using the relationship between the different Green's functions: $G^r - G^a = G^> - G^<$ (c.f. Appendix C), Eq. 15 can be rewritten as $J_L = e/h \int d\omega \text{Tr} \{ \Sigma_L^<(\omega) G^>(\omega) - \Sigma_L^>(\omega) G^<(\omega) \}$, where the self-energies due to the coupling of the central region to the left lead are $\Sigma_L^< \propto i f_L \Gamma_L$ and $\Sigma_L^> \propto -i(1 - f_L) \Gamma_L$. The physical interpretation of this equation is more transparent than Eq. 15. The first term gives the current flowing through the left contact from the left electrode towards the central region, because it includes $G^>$ which gives information about the empty non-equilibrium states in the central region and the self-energy $\Sigma_L^<$ which is proportional to the distribution of occupied states in the left lead. The second term gives the current flowing through the left contact towards the electrode because it includes $G^<$ which gives information about the occupied non-equilibrium states of the central region, and the self-energy $\Sigma_L^>$ is proportional to left lead empty states.

Now, to get physical results for the current we need to calculate the different Green's functions involved in Eq. 15. These functions obey Dyson-like equations $G^{r,a} = G_0^{r,a} + G_0^{r,a} \Sigma^{r,a} G^{r,a}$ for $G^{a,r}$ and another quantum kinetic equation for $G^{<,>}$, i.e. $G^{<,>} = (1 + G^r \Sigma^r) G_0^{<,>} (1 + \Sigma^a G^a) + G^r \Sigma^{<,>} G^a$. The first term in the equation for $G^{<,>}$ comes from the initial conditions and is seen as a boundary condition. It is generally omitted for the stationary-state since it acts only in the transient regime. The approach is now very useful if we can construct the self-energy functionals that include the physics of the many-body system considered and that a sufficiently good solution can be obtained from the coupled equations for $G^{a,r}$ and $G^{<,>}$ (c.f. Appendix C). One important point is that the self-energy functionals and the solution obtained for the Green's functions preserve the condition of current conservation. It can be shown that within the decomposition made above for the different kinds of interaction, the condition for current conservation requires that $\int d\omega \text{Tr} \{ \Sigma_{\text{inel}}^<(\omega) G^>(\omega) - \Sigma_{\text{inel}}^>(\omega) G^<(\omega) \} = 0$, where $\Sigma_{\text{inel}}^{<,>}$ are the self-energies due to interactions of types (i) and (ii) as defined above. This condition says that what is inelastically scattered into the central region should compensate what is inelastically scattered out of the central region. It is not obvious that all choices for the self-energy functionals fulfil this condition. A good example is the SCBA for the electron-phonon interaction calculated from the undressed phonon Green's function D_0 . The SCBA has been used recently to study the effects of the coupling between electrons and atomic motion in atomic wires [103, 104]. Other self-energy functionals, developed in the spirit of the SCBA and including more elaborate approximations for the phonon propagators, have also been used to study the effects of the interaction between electrons and atomic vibrations in model systems [42, 105–110] and in more realistic atomic and molecular wires [111–116]. However the problem of non-equilibrium transport through a coupled electron-phonon system is very complex to solve exactly, and more work towards this direction needs to be done.

Quantum kinetic equations: It is possible to derive a quantum analog to the Boltzmann semiclassical equation for transport from the non-equilibrium Green's functions. The detailed derivation is rather complex and has been well described in other review articles [100, 117, 118]. Here we summarise the principles for obtaining such quantum kinetic equations.

We start with the lesser Green's function $G^<$ given in a space-time representation (r, t) for a fermion field operator in a solid. Then we perform a transformation similar to that given in Appendix B by defining the centre-of-mass and time-average coordinates $(R, T) \equiv \frac{1}{2}(r_1 + r_2, t_1 + t_2)$ and the relative coordinates $(x, \theta) \equiv (r_1 - r_2, t_1 - t_2)$. The Green's function $G^<(r, \theta; R, T)$ expressed in these new coordinates is Fourier transformed in space and time with respect to the relative coordinates to give $G^<(k, \omega; R, T)$, from which is defined the so-called Wigner distribution function $f(k, \omega; R, T) = iG^<(k, \omega; R, T)$. The distribution $f(k, \omega; R, T)$ is the quantum analog of the semiclassical distribution function $f(r, v, t)$ used in the Boltzmann equation for transport (v being the particle velocity at point (r, t))[‡]. In a system governed by the laws of quantum mechanics, because of the uncertainty principle and because scattering smears out the energy and momentum states, the usual relation between energy and velocity does not hold any more. Thus we have to consider a distribution function of the type $f(k, \omega; R, T)$ where the energy ω and momentum k are treated as independent variables.

In order to get the quantum Boltzmann equation, we write the equation of motion for the Green's function $G^<(k, \omega; R, T)$. This is the most difficult part of the problem especially when we want to treat a many-body system with interactions [117, 118]. However the quantum distribution function $f(k, \omega; R, T)$ is the only correct distribution function to describe particles in an interacting, many-body approach. In the presence of an electric field, the following quantum Boltzmann equation can be derived [117]

$$\frac{\partial}{\partial t} f + v \cdot \nabla_r f + F \cdot \left\{ \frac{\nabla_k}{m} + v \frac{\partial}{\partial \omega} \right\} f + \left(\frac{\partial}{\partial t} f \right)_S = 0, \quad (17)$$

where F is the force (electric field) acting on the electron. An additional driving term $(v \cdot F \partial f / \partial \omega)$ is obtained in comparison to the usual Boltzmann equation. The last term $(\partial f / \partial t)_S$ arises from the inelastic scattering due to interaction between particles. It can be calculated by the use of self-energies $\Sigma(\omega)$ (arising from electron-electron or electron-phonon interactions) in the corresponding equation of motion for $G^<(k, \omega; R, T)$. Once Eq. 17 is solved for the distribution function $f(k, \omega; R, T)$, we can calculate the macroscopic quantities, as measured in various experiments, such as the electronic density $n(R, T)$, the electronic current $j(R, T)$, the energy density $n_E(R, T)$ and energy current $j_E(R, T)$. The latter are obtained from the different moments (in energy ω or momentum k) of the distribution function f . Finally, the semiclassical Boltzmann distribution $f(R, v, T)$ is found by integrating the distribution function $f(k = mv, \omega; R, T)$ over energy.

3.3. Molecular dynamics based methods

There have been many suggested ways to modify the standard Born-Oppenheimer based molecular dynamics algorithms. It is usual to speak of their being broad categories of methods: surface hopping and effective interaction. The former category is very popular for studies of molecular systems, but has well-known deficiencies (it is somewhat *ad hoc*, and coherence between trajectories is lost). The latter approach (usually in the Ehrenfest approximation) is popular for some problems but also has

[‡] Note that the function $f(k, \omega; R, T) = iG^<(k, \omega; R, T)$ is related to the Wigner matrix used in CEID (see section 3.3.4) by an integral over the energy ω [119]. However, as used in CEID the transform is over nuclear degrees of freedom, while here it is over electronic ones.

limitations. One recent method (Correlated Electron-Ion dynamics [120–123]) sits somewhere between the two usual categories, though it is viewed as an extension of the Ehrenfest approximation. We begin with a discussion of the Ehrenfest method because of its importance as a starting point for the other methods. We then present alternative methods that attempt to overcome its deficiencies.

3.3.1. Ehrenfest method This is a simple, but ingenious, method that successfully adds some non-adiabatic features to molecular dynamics, but is incomplete. There are many ways to derive the formal equations for this method, but the one we shall use here most naturally leads us to CEID which is discussed in detail below.

The Ehrenfest method consists of two separate approximations: the electrons interact with the nuclei through a classical field generated by its charge distribution (a mean field approximation, and the main source of error); the nuclei obey classical (Newtonian) mechanics. We will work with the density matrix.

The first approximation allows us to write the full density matrix $\hat{\rho}$ as a tensor product of an electron density matrix $\hat{\rho}_e$ and a nuclear density matrix $\hat{\rho}_N$: $\hat{\rho} = \hat{\rho}_e \otimes \hat{\rho}_N$. If we substitute this into the quantum Liouville equation

$$\frac{d\hat{\rho}}{dt} = \frac{1}{i\hbar} [\hat{H}, \hat{\rho}] \quad (18)$$

and then trace out either the nuclear or electronic degrees of freedom we obtain the following equations of motion:

$$\begin{aligned} \frac{d\hat{\rho}_e}{dt} &= \frac{1}{i\hbar} [\bar{H}_e, \hat{\rho}_e] \\ \frac{d\hat{\rho}_N}{dt} &= \frac{1}{i\hbar} [\bar{H}_N, \hat{\rho}_N] \end{aligned} \quad (19)$$

where $\bar{H}_e = \text{Tr}_N \{ \hat{H}_e \hat{\rho}_N \}$, $\bar{H}_N = \hat{T}_N + \text{Tr}_e \{ \hat{H}_e \hat{\rho}_e \}$, $\text{Tr}_N \{ \dots \}$ means a trace over nuclear coordinates, and $\text{Tr}_e \{ \dots \}$ means a trace over electronic coordinates. The total Hamiltonian (\hat{H}) has been separated into the nuclear kinetic energy (\hat{T}_N) and the rest (\hat{H}_e). It is the presence of the traces in the definitions of the effective Hamiltonians that results in the electrons and nuclei only responding to the classical fields. Note that below we show how the Ehrenfest approximation can lift the mean field approximation for the nuclei because they can be treated as classical particles with unique trajectories.

The classical nature of the nuclei is introduced by replacing the quantum commutator brackets by classical Poisson brackets. The equation of motion for the classical nuclear density matrix (now a phase space density) becomes

$$\frac{d\rho_N(\vec{R}, \vec{P})}{dt} = \sum_{\nu} \left(\frac{\partial \bar{H}_N(\vec{R})}{\partial R_{\nu}} \frac{\partial \rho_N(\vec{R}, \vec{P})}{\partial P_{\nu}} - \frac{P_{\nu}}{M_{\nu}} \frac{\partial \rho_N(\vec{R}, \vec{P})}{\partial R_{\nu}} \right) \quad (20)$$

where R_{ν} and P_{ν} are the position and momentum coordinates and M_{ν} is a nuclear mass. If we consider just a single classical trajectory (indicated by the subscript T) then we have:

$$\rho_N(\vec{R}, \vec{P}) = \prod_{\nu} \delta(R_{\nu} - R_{T,\nu}(t)) \delta(P_{\nu} - P_{T,\nu}(t)) \quad (21)$$

where $R_{T,\nu}(t)$ and $P_{T,\nu}(t)$ are the nuclear positions and momenta along the trajectory. Substituting Eq. 21 into Eq. 20 we obtain

$$\dot{R}_{T,\nu} = \frac{P_{T,\nu}}{M_{\nu}}$$

$$\dot{P}_{T,\nu} = - \frac{\partial \bar{H}_N(\vec{R}_T)}{\partial R_{T,\nu}} = -\text{Tr}_e \left\{ \hat{\rho}_e \frac{\partial \hat{H}_e(\vec{R}_T)}{\partial R_{T,\nu}} \right\} \quad (22)$$

Inserting this nuclear density (Eq. 21) into the equation of motion for the electrons (Eq. 19) we obtain

$$\frac{d\hat{\rho}_e}{dt} = \frac{1}{i\hbar} [\hat{H}_e(\vec{R}_T), \hat{\rho}_e] \quad (23)$$

Equations 22 and 23 constitute the Ehrenfest approximation. The use of a *single* nuclear trajectory in fact takes us halfway to introducing microscopic fluctuations: the electrons now respond to *individual* nuclei. However, the converse is not true, with the nuclei still responding to an average distribution of electrons.

This approximation can fail either when the nuclei have to be treated as quantum particles (for example, when tunnelling takes place), or the nuclei respond to the microscopic fluctuations in the electron charge density as well as the mean (for example, Joule heating). In this review we are principally concerned with the latter case.

To make this more transparent, let us suppose that the electronic density matrix can be represented by a phase space distribution $\rho_e(\vec{r}, \vec{p})$ (this can be formally justified by means of the Wigner transform as described in Appendix B). In this case we have $\bar{H}_N(\vec{R}) = \int d\vec{r} d\vec{p} \rho_e(\vec{r}, \vec{p}) H_e(\vec{R}; \vec{r}, \vec{p})$, and hence the force on the nuclei (\bar{F}_ν) due to the electrons and the other nuclei is (Eq. 22) $\bar{F}_\nu = - \int d\vec{r} d\vec{p} \rho_e(\vec{r}, \vec{p}) \partial H_e(\vec{R}; \vec{r}, \vec{p}) / \partial R_\nu$. If, as for the nuclei, we could isolate a *single* electronic trajectory $\vec{r}_T(t)$, then the force would just be $\bar{F}_\nu = -\partial H_e(\vec{R}; \vec{r}_T, \vec{p}_T) / \partial R_\nu$. The integral, then, gives the average force produced by a *set* of trajectories with each one contributing to the force with a weight $d\vec{r} d\vec{p} \rho_e(\vec{r}, \vec{p})$.

This averaging has the effect of reducing the ability of electrons to pass energy to the nuclei. To understand this, consider the following simple model. Suppose we have one nucleus that experiences forces from the electrons that have two contributions: $\vec{F} = -k\vec{X} + \vec{f}(t)$. The first, harmonic, term corresponds to motion on a Born-Oppenheimer surface. The small residual non-adiabatic corrections are represented by the force $\vec{f}(t)$. Let us define the energy of the nucleus as $U_N = P^2/2M + kX^2/2$. The rate change of this energy (the power given to the nucleus) satisfies $\dot{U}_N = \vec{X} \cdot \vec{f}(t)$. If we now evaluate the average power supplied over some time interval τ we obtain

$$\langle \dot{U}_N \rangle_\tau = \frac{1}{\tau} \int_{t_0}^{t_0+\tau} \vec{X} \cdot \vec{f}(t) dt \quad (24)$$

If $\vec{f}(t)$ varies only slightly during a vibrational period of the nucleus, then the power will be very small, as the average velocity of the nucleus is zero. If it fluctuates rapidly but there are no correlations between \vec{X} and \vec{f} , then the fluctuations average out and the power again vanishes. However if we allow \vec{X} to be a functional of \vec{f} , via the equation of motion, then in Eq. 24 there are correlated force-velocity fluctuations, which can in turn be expressed in terms of the force-force correlation function [51]. It is these correlated fluctuations that generate the power. This result is known as the fluctuation-dissipation theorem. The effect of the averaging over electronic trajectories in the Ehrenfest approximation is to break the microscopic correlations between the force experienced by the nucleus due to the electrons and the momentum of the nucleus, and thus to suppress the energy that can be transferred to the nucleus.

This breaking of correlation is caused by the averaging of the electronic trajectories for every nuclear configuration.

The above analysis is most natural for metallic systems which we can think of as nuclei embedded in a gas of rapidly moving light electrons. For small molecules with well spaced energy levels the criticism of the Ehrenfest approximation can be made differently. The calculations usually involve an electronic transition between two levels, induced by the momentum of the nuclei. It is found that the results are often in poor agreement with accurate quantum calculations. This is explained by noting that the single nuclear trajectory experiences forces simultaneously from a number of partially occupied energy surfaces, whereas it should be experiencing it from one only, but with separate trajectories on each surface. This is just another manifestation of the averaging discussed above.

These problems manifest themselves in the failure to produce certain outcomes in simulations, such as heating of nuclei by current carrying electrons [51], thermal equilibrium between electrons and nuclei [124, 125], and correct transition probabilities [126]. Various schemes have been proposed to overcome these problems. One starting point is to recognise that the ionic wavefunction rapidly decoheres after a transition leading to modified equations of motion [127–129], or to a stochastic algorithm in which trajectories on separate Born-Oppenheimer energy surfaces are treated as independent (see Section 3.3.2 below). Another is to treat the electrons and nuclei as having correlated motion leading to wavepacket-like methods [130, 131] (see Section 3.3.4 below).

While the Ehrenfest approximation is often presented in the literature as a straw man (that is, a method used simply to show how much better other methods are), it is also used to obtain useful results. Two applications are:

- (i) Time-dependent density functional theory has been used successfully to study the friction forces experienced by hydrogen atoms scattering off a metallic surface [132]. The friction is due to the excitation of electrons by the moving atoms. Energy transfer in this direction is correctly described by the Ehrenfest approximation.
- (ii) Polymers have been successfully studied quite extensively using the Ehrenfest approximation within a simple tight binding model for the electrons. Investigations have included: polaron drift in an applied electric field [133]; the dynamics of polarons formed after the excitation of electrons by photons [134]; the nucleation of stable self-localised excitations [135].

3.3.2. Surface hopping methods Surface hopping was originally proposed by Tully and Preston [136] as a phenomenological extension of the classical trajectory method which incorporates non-adiabatic effects. In the classical trajectory method, an ensemble of trajectories sampling a series of initial conditions for a gas phase chemical reaction is integrated in time. Quantities such as reaction cross sections are obtained as averages over the ensemble.

As mentioned in the previous section, within the Ehrenfest approximation nuclei feel a force from the electrons that is an average over many electronic trajectories. In cases where adiabatic electronic states are close to each other in energy over relatively small regions of space and are well separated otherwise, as in the case of a non-adiabatic chemical reaction, when the nuclei leave a region of strong coupling the force felt by them is a weighted average of the force in each surface. Tully and

Preston observe that "*intuition requires that the motion take place on one surface or the other*". That is, after going through a region where there is significant coupling between surfaces the ions must stay on the original surface on which they were moving or jump to a different one. This intuition is guided by the fact that in a molecular beam experiment, reactants convert to one set of products or the other, but one does not detect states which are mixture of different product channels. This implies some decoherence of any mixed state before the outcome is measured (or during the measurement), which in turn suggests a picture of the dynamics in which nuclei move adiabatically unless they encounter a region of strong non-adiabatic coupling. This can be either a point where adiabatic surfaces cross or where they are close in energy.

This idea was implemented into the first realization of the surface hopping procedure by determining a fixed region or set of points in configuration space where switching between adiabatic states is likely. When the system passes through those regions during the dynamics the decision to hop to a different surface is taken according to a probability calculated from the Landau-Zener expression (see section 3.2.1). After a jump to a different potential energy surface has taken place, the nuclei change their potential energy by a finite amount, which is small if the jump occurs when the two surfaces are close to each other. In order to conserve energy the surface hopping procedure must be complemented with a prescription on how to change the velocities of the nuclei after a hop. In their original proposal, Tully and Preston rescaled the velocities in one particular direction, chosen from the topology of the potential energy surface and the calculated couplings. As with the standard classical trajectory method, properties of interest are calculated from the properties of an ensemble of integrated trajectories.

Tully later extended the method by lifting the constraint of fixed hopping regions and named the new method Molecular Dynamics with Quantum Transitions (MDQT) [137, 138]. In this method, the jumps between surfaces can occur at any point during the trajectory. The decision whether a hop should occur and to which surface is taken according to a probability of a jump occurring. This is calculated from the time evolving state populations, which in turn is obtained from the simultaneous integration of the nuclear dynamics on a certain adiabatic potential energy surface and the equation of motion for the electronic wave function or density matrix. This starts by recasting the equations for Ehrenfest dynamics given before in terms of the adiabatic electronic states (see section Appendix A). First, the following anzatz is made for the electronic wavefunction

$$\Psi(t) = \sum_j c_j(t) \Phi_j(\vec{R}(t))$$

where $\Phi_n(\vec{R}(t))$ are the adiabatic eigenstates of the instantaneous electronic Hamiltonian, and are a function of time via the nuclear coordinates. Replacing this ansatz in the Schrödinger equation for the electrons we obtain the following equation of motion for the electronic wavefunction coefficients:

$$i\hbar \dot{c}_j = c_j E_j(\vec{R}(t)) - i\hbar \sum_k c_k \vec{R} \cdot \vec{d}_{kj} \quad (25)$$

where the *non-adiabatic coupling vector* \vec{d}_{kj} is defined by

$$\vec{d}_{kj} = \int \Phi_k^*(\vec{R}(t)) \nabla_{\vec{R}} \Phi_j(\vec{R}(t)) d\vec{R}.$$

The same result can be obtained via a variational procedure from a suitably constructed Lagrangian [139]. The second term in Eq. 25 is the one responsible for transitions between states. This transitions will be more effective if the nuclear velocity points in the direction of the non-adiabatic coupling vector. The rate of change of the population on a given state is given by the equation of motion for a diagonal element of the electronic density matrix:

$$\dot{\rho}_{ii} = -i\hbar \sum_j 2\text{Re} \left\{ \rho_{ij} \vec{R} \cdot \vec{d}_{ij} \right\} = \sum_j b_{ij} \quad (26)$$

Where we have taken into account the fact that the matrix of non-adiabatic coupling vectors is anti-hermitian. The fewest switches algorithm proposed by Tully was designed so that the choice of where to hop resembles the kinetic Monte Carlo integration of a master equation for the state occupations given by Eq. 26. In a given time step the probability that a trajectory occupying state i hops to a different state j is proportional to b_{ij} . This probability is constrained in a way that minimizes the number of hops required to achieve consistency between the occupations and the number of trajectories in the ensemble that occupy a given state. Tully demonstrates that the algorithm ensures that at any time the number of trajectories in a given state is representative of the occupation of that state. However, the problem with this argument is that there is no unique set of occupations, but instead there is one for each trajectory. If the occupations of the states from different trajectories diverge fast relative to one another because the nuclei follow different paths (something that will occur faster the more hops there are) then consistency will be lost [140].

In order to conserve energy whenever a hop occurs the velocity component pointing in the direction of the non-adiabatic coupling vector is rescaled. If, from the algorithm, it is determined that a hop must occur to a potential energy surface for which there is not enough energy, the hop is aborted and the velocity in the direction of the non-adiabatic coupling vector is reversed [138]. These classically forbidden hops can become a problem if they occur too often since they contribute to breaking the consistency between the propagated occupations and the number of trajectories in a given state [140].

Comparison with fully quantum results for simple systems shows that the method produces qualitatively correct results [137, 141]. Unlike the Ehrenfest method it reproduces the correct Boltzman populations when the system is coupled to a thermostat [125]. The fact that for each particular trajectory a full quantum wavefunction is propagated means that the method accounts in some way for coherence within each trajectory and some effects due to interference can be reproduced [137]. However no interference exists between trajectories. Further, it is difficult to asses, because of the way in which the interaction between nuclear and electronic degrees of freedom is treated, whether the resulting quantum coherence effects are meaningful [142]. One particular problem is the fact that the method seems to work only when the electronic states are represented in an adiabatic basis [143]. This is probably due to the fact that the use of this basis leads to the least number of hops [144]. The rescaling of the velocity after a hop, which is another controversial feature of surface hopping, can be justified in a number of ways by semiclassical arguments [145, 146]. Although the replacement of the propagation of a single, fully coherent, wavefunction by an ensemble of trajectories can be made plausible by semiclassical arguments [143] some aspects of the method are clearly *ad hoc* making it difficult to improve in a systematic way, or to predict in which situations it can be applied successfully.

Extensions of the method exist for cases in which there are both discrete and continuum states [147]. They either use different schemes to choose when to hop [148] or replace sudden hops by a continuous switching [149]. Prezhdo and Rossky proposed a combination of the Ehrenfest and surface hopping procedures in which the force used to propagate the nuclear trajectory comes from the integration of Ehrenfest equations, not just one adiabatic state, but this wavefunction is reduced to a single adiabatic state when a hop occurs or when the validity of the Ehrenfest approximation is violated according to some pre-established criteria [150].

Tully's MDQT is one of the most used methods to deal with problems in which coupling between electrons and ions is fundamental. In particular, it has been extensively used to study non-adiabatic processes in liquids, given that the complexity of liquid structure prevents application of other techniques. One of the first applications of the method was to the problem of the solvated electron. Space and Coker explored the relaxation of an excess electron in dense fluid helium. MDQT provided information on the dependence of the electronic relaxation process on the initial electronic state [151]. Later, MDQT and some of its variants were applied to an excess electron in water [152–154]. Another classical problem to which the method has been applied is the simplest photochemical reaction in solution, photodissociation of a diatomic molecule. Coker's group pioneered the application of MDQT to this problem, studying the photodissociation of I_2 in liquid and solid rare gases [155, 156]. Others later studied photodissociation of diatomic molecules embedded in rare gas clusters [157, 158]. The case of the ICN molecule which can isomerize after dissociation has been studied in rare gas matrices [159], where some of the vibrational modes of the molecule were included within the quantum description, in bulk water [160] and at the liquid/vapour interface of water [161]. An important effect of the solvent in the case of photodissociation is that some processes which occur with high quantum yields in the gas phase are inhibited in the solvent. This effect is explained in terms of the caging of the reactants which are held together in the solvent and have the opportunity to recombine. Particularly dramatic is the case of azomethane (H_3CNCH_3) which photodissociates in the gas phase but isomerizes around the NN double bond in the solvent. This problem was studied using surface hopping in the group of Persico [162–164], becoming one of the first non-adiabatic simulations of condensed phase photochemistry with a realistic solvent and a polyatomic solute. Since photodissociation is a classic problem in photochemistry, there are abundant experimental results for these systems which can be compared with the results obtained from the simulations. In general the agreement has been found to be good.

Relaxation of a charge transfer excited state via intramolecular electron transfer in solution is another classic example of a non-adiabatic problem in solution chemistry. Lobaugh and Rossky studied the relaxation of excited betaine in acetonitrile. The electronic structure of the molecule was described using configuration interaction applied to a simple semiempirical model [165]. The authors found that besides the motion of the solvent, which is effective during the initial stages of the relaxation from the excited state, also some internal motions of the molecule played a fundamental role in the relaxation process.

Photoisomerization around a double bond is a paradigmatic example of non-adiabatic chemistry, and important biological functions such as vision hinge on it. Surface hopping has been used to study the photoisomerization of butadiene [166], the chromophore of the photoactive yellow protein [167] and of retinal in bacteriorhodopsin [168]. Azobenzenes are one class of compounds that can be used for the generation of

materials which change their properties via illumination. *Trans* to *cis* isomerization of azobenzene is the key for this effect, and surface hopping has recently been used to solve some controversy on the detailed mechanism of the process [169].

Very few applications of surface hopping to processes in solids exist. Yokozawa and Miyamoto studied the breaking of Si-H bonds from H terminated O vacancies in SiO₂ by hot electrons using a primitive combination of the surface hopping procedure and first principles molecular dynamics [170]. Bruening and Friedman used surface hopping and a tight binding Hamiltonian to describe charge transfer from a conducting polymer to C₆₀ molecules [171]. Bach and Gross treated with surface hopping the problem of charge transfer in molecule-surface scattering [144].

An important difficulty with the implementation of surface hopping procedures is the need for accurate adiabatic states and non-adiabatic coupling vectors which must be obtained from some model description of the electronic structure or as a parametrization of *ab initio* results prior to the simulation. Recently, surface hopping has been implemented in *ab initio* molecular dynamics methods with on the fly calculation of the electronic structure. Doltsinis and Marx have implemented surface hopping within a restricted open-shell Kohn-Sham scheme [172] which allows the calculation of the low lying excited states and the corresponding coupling vectors between states [173]. The method was applied to *cis-trans* photoisomerization of formaldimine (H₂CNH) [173], excited state proton transfer and internal conversion of *o*-hydroxybenzaldehyde [174], and the photostability of methylated DNA bases [175]. Prezhdo *et al.* have implemented a similar scheme where the adiabatic states used for the surface hopping propagation are different excited Kohn-Sham determinants and applied the method to study the nonradiative relaxation of the chromophore of the green fluorescent protein and electron injection from alizarin into titanium dioxide [176].

Recently, some new formulations of surface hopping techniques have appeared which are constructed from well defined approximations of the exact quantum dynamics [177–179]. These techniques have up to now been demonstrated to produce excellent results when compared with exact calculations for model systems, and some small problems [178]. Perhaps in the future these formally correct methods will become available for realistic condensed phase systems.

3.3.3. Frozen Gaussian Approximation and related methods In this section, we will cover the Frozen Gaussian approximation (FGA) and various related semiclassical (SC) techniques including the Initial Value Representation (IVR) and the Herman-Kluk propagator. We will also consider methods which use the FGA for nuclear wavefunctions (one of these, surface hopping, which sometimes uses FGA for the nuclei is discussed in Section 3.3.2). There are various other reviews of these techniques which go into more detail: a thorough, though very formal, review of semiclassical methods [180]; an overview of SC-IVR methods [181]; a discussion of wavepacket (FGA) and surface hopping methods [182]; and a more general review covering time dependent methods for large systems [183].

The use of gaussian wavepackets as a basis for nuclear wavefunctions started in scattering calculations which relegated the electrons to the role of providing a potential; their use was pioneered by Heller [184–189]. From this work, he proposed that a simple way to broaden single classical trajectories would be to use a Gaussian function whose width was fixed and whose average position and momentum followed that trajectory [190]. For a gaussian centred on the phase-space point (\mathbf{r}, \mathbf{p}) with

width γ , we write:

$$\langle \mathbf{x} | \mathbf{r}, \mathbf{p} \rangle = \left(\frac{2\gamma}{\pi} \right)^{N/4} \exp \left[-\gamma(\mathbf{x} - \mathbf{r})^2 + i\mathbf{p} \cdot (\mathbf{x} - \mathbf{r})/\hbar \right] \quad (27)$$

The semiclassical approximation (due originally to Van Vleck [191] as an extension of the WKB method to time-dependent problems) provides a way to address dynamics. Consider the amplitude to change from state 1 to state 2 for a system with continuous position and momentum (\mathbf{r}, \mathbf{p}) :

$$T_{1 \rightarrow 2} = \langle \Psi_2 | e^{-i\hat{H}t/\hbar} | \Psi_1 \rangle = \int \int d\mathbf{r}_1 d\mathbf{r}_2 \Psi_2^*(\mathbf{r}_2) \langle \mathbf{r}_2 | e^{-i\hat{H}t/\hbar} | \mathbf{r}_1 \rangle \Psi_1(\mathbf{r}_1) \quad (28)$$

The semiclassical approximation changes the propagator to:

$$\begin{aligned} \langle \mathbf{r}_2 | e^{-i\hat{H}t/\hbar} | \mathbf{r}_1 \rangle &= \sum_{\text{roots}} C e^{iS(\mathbf{r}_2, \mathbf{r}_1)/\hbar} \\ S(\mathbf{r}_2, \mathbf{r}_1) &= \int_0^t dt' (T(t') - V(t')) \end{aligned} \quad (29)$$

Here $S(\mathbf{r}_2, \mathbf{r}_1)$ is the classical action for the trajectory going from \mathbf{r}_1 to \mathbf{r}_2 in time t ; this makes clear the connection to Feynman's path-integral formulation of quantum mechanics. The factor C contains a number of factors which there is not space to discuss here (see for instance Ref. [181, 192]). The sum over roots arises from the stationary phase limit [193] which gives all classical paths for which $\delta S = 0$. Solving this equation as written gives a non-linear boundary value problem, where all values of \mathbf{p}_1 which yield \mathbf{r}_2 must be found; this will lead, in general, to multiple roots.

The initial value representation replaces the integration over final coordinates, $d\mathbf{r}_2$, with integration over initial momenta, $d\mathbf{p}_1$ (bringing in a Jacobian with the change of variables). The sum over roots also disappears because the initial conditions determine a unique classical trajectory. We can write:

$$\sum_{\text{roots}} \int d\mathbf{r}_2 = \int d\mathbf{p}_1 \left| \frac{\partial \mathbf{r}_2}{\partial \mathbf{p}_1} \right| \quad (30)$$

This approximation allows some quantum interference and tunnelling effects to be described, while involving only real, classical trajectories.

The most commonly used combination of a Frozen Gaussian basis, and the semiclassical IVR is the Herman-Kluk propagator [194, 195].

$$\begin{aligned} \psi(\mathbf{x}, t) &= \int \frac{d^N \mathbf{r}_i d^N \mathbf{p}_i}{(2\pi\hbar)^N} \langle \mathbf{x} | \mathbf{r}_t, \mathbf{p}_t \rangle C(\mathbf{r}_i, \mathbf{p}_i, t) \\ &\times \exp [iS(\mathbf{r}_i, \mathbf{p}_i, t)/\hbar] \langle \mathbf{r}_i, \mathbf{p}_i | \psi_0 \rangle, \end{aligned}$$

for an N -dimensional problem. A trajectory starts at phase space point $(\mathbf{r}_i, \mathbf{p}_i)$ and runs for time t to a phase space point $(\mathbf{r}_t, \mathbf{p}_t)$. The form of the semiclassical prefactor required is important if the calculation is to be carried over long time periods [195]:

$$C(\mathbf{r}_i, \mathbf{p}_i, t) = \left| \frac{1}{2} \left(\frac{\partial \mathbf{p}_t}{\partial \mathbf{p}_i} + \frac{\partial \mathbf{r}_t}{\partial \mathbf{r}_i} - 2\gamma i\hbar \frac{\partial \mathbf{r}_t}{\partial \mathbf{p}_i} + \frac{i}{2\gamma\hbar} \frac{\partial \mathbf{p}_t}{\partial \mathbf{r}_i} \right) \right|^{1/2} \quad (31)$$

The SC wavepacket methods described thus far have the important features of time-reversal and unitarity [196]. However, in their original form, there are often rapid oscillations in the integrand which cause problems with convergence. These oscillations were shown to be significantly damped [197] by the merging of the cellular

dynamics method [198] with the Herman-Kluk propagator. Other solutions to this problem include time integration over short periods [199] yielding effective averaging over the short period. Still within the realm of reactive scattering, the limitations of the Herman-Kluk propagator have been explored in 2D and 4D modelling of H₂ scattering from Cu(001) [200]. The 2D simulation was not sufficiently accurate, while the full 4D simulation required inordinate amounts of computational effort. There has been application to non-adiabatic electronic evolution, in particular to the canonical problem of electron solvation [201]. In this area, FG propagation coupled with perturbation theory has been compared to the surface-hopping techniques [202]. In regimes where tunnelling is important, surface hopping is less accurate, though the FG propagation is only accurate over short timescales, and can depend on the width chosen for the Gaussian. Some analysis of the accuracy of using classical mechanics for the propagation of the wavepackets in condensed many-body systems [203] showed that while the wavefunction can spread (losing the justification for the FGA), densities continue to be localised, due to interference effects. These ideas have been applied to the calculation of non-linear optical response functions, with reasonable accuracy [204]. These SC-IVR methods scale exponentially with the number of degrees of freedom [205] though this does depend on the number of final states contributing and the energy resolution required.

In order to model non-adiabatic transitions, the FGA (and any SC-IVR) must be extended. It has been shown [192, 206] that it is possible to linearise the SC-IVR [207], splitting the entire system into a system and a bath; and expansion is then made in terms of the bath coordinates, using Wigner distributions. This technique has been applied to simple models (a Morse oscillator coupled to a single harmonic mode) [192], and the spin boson problem with different spectral weights [206, 208], with good agreement to exact results.

The multiple-spawning technique [209–211] uses frozen Gaussians as basis functions during a time-dependent simulation. An effective non-adiabatic coupling is monitored between two states I and I' ; using a diabatic (see Appendix A) representation for the electronic wavefunctions, this can be written as :

$$d(\mathbf{R}) = \left| \frac{\langle I | \hat{H} | I' \rangle}{V_{II}(\mathbf{R}) - V_{I'I'}(\mathbf{R})} \right| \quad (32)$$

When this coupling for state I exceeds a threshold, new nuclear wavefunctions are added (or *spawned*) on the new state I' at a constant rate (so that more wavefunctions are added the longer the system remains in the area of non-adiabatic coupling). These new functions are then propagated, and can themselves spawn. This leads to a system whose nuclear degrees of freedom follow multiple trajectories on different surfaces simultaneously. It has been applied successfully, among other things, to a two dimensional non-reactive collision [211], and more recently to light-driven reactions [212].

The Zhu-Nakamura (ZN) theory [57] for non-adiabatic transitions (an extension of the Landau-Zener formalism that works with adiabatic states) has been combined with the use of frozen Gaussians for the nuclear wavefunctions [213–215] to extend both theories, both with the surface hopping formalism [213, 214] (specifically using ZN theory to calculate the non-adiabatic transitions) and as a separate method [215]. This approach has the advantage of giving the rates from an analytic theory, while allowing nuclear wavefunction propagation, and works well in multidimensional problems (by comparison to more complicated and costly numerical calculations of the problems).

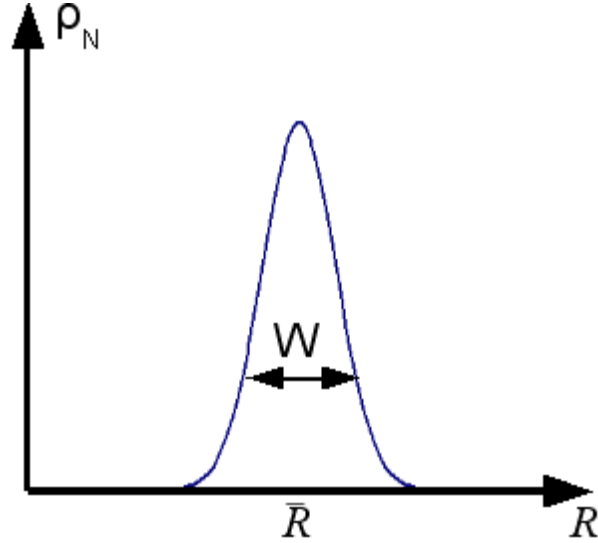


Figure 3. The central idea in correlated electron ion dynamics is that the width of a nuclear wave packet is narrow on the length scale of the separation between nuclei. That is, $W \ll d$ where d is a typical distance between nuclei. In this figure the mean density of the nuclei as a function of position R is given the symbol ρ_N . Correlations between the electrons and nuclei are maintained by allowing the electronic state to vary as a function of position of the nuclei within the wave packet.

3.3.4. Correlated electron-ion dynamics The small amplitude moment expansion is a scheme to introduce the correlations between the electronic fluctuations and the nuclei that are missing in the Ehrenfest approximation [51]. When this expansion is combined with molecular dynamics, we refer to it as Correlated Electron-Ion Dynamics (CEID). The starting point is the Ehrenfest equations (which are, of course exact, and which give the name to the approximation):

$$\begin{aligned}\dot{\bar{R}}_\nu &= \frac{\bar{P}_\nu}{M_\nu} \\ \dot{\bar{P}}_\nu &= \bar{F}_\nu \\ \bar{F}_\nu &= - \text{Tr} \left\{ \hat{\rho} \frac{\partial \hat{H}_e}{\partial \hat{R}_\nu} \right\}\end{aligned}\tag{33}$$

where $\bar{R}_\nu = \text{Tr} \{ \hat{R}_\nu \hat{\rho} \}$ and $\bar{P}_\nu = \text{Tr} \{ \hat{P}_\nu \hat{\rho} \}$, and \hat{R}_ν and \hat{P}_ν are the position and momentum operators for the nuclei. In the Ehrenfest approximation we were able to work with a single trajectory: in that case $\bar{R}_\nu = R_{T,\nu}$ and $\bar{P}_\nu = P_{T,\nu}$. However, since the Ehrenfest equations refers to quantum nuclei, the uncertainty principle makes it impossible to have individual trajectories. The best we can manage are narrow wave packets (see figure 3). In this case \bar{R}_ν and \bar{P}_ν correspond to the trajectory of the mean of the wave packet.

If the wave packets really are narrow (which they often are in condensed systems), then we can expand $\hat{H}_e(\hat{R})$ about \bar{R} in the following way [120] (where \hat{R} and \bar{R} stand

for the set of coordinates $\{\hat{R}_\nu\}$ and $\{\bar{R}_\nu\}$ respectively):

$$\hat{H}_e(\hat{R}) = \hat{H}_e(\bar{R}) + \sum_\nu \Delta \hat{R}_\nu \frac{\partial \hat{H}_e(\bar{R})}{\partial \bar{R}_\nu} + \frac{1}{2} \sum_{\nu\nu'} \Delta \hat{R}_\nu \Delta \hat{R}_{\nu'} \frac{\partial^2 \hat{H}_e(\bar{R})}{\partial \bar{R}_\nu \partial \bar{R}_{\nu'}} + \dots \quad (34)$$

where $\Delta \hat{R}_\nu = \hat{R}_\nu - \bar{R}_\nu$. Then the mean force (Eq. 33) satisfies

$$\bar{F}_\nu = -\text{Tr}_e \left\{ \hat{\rho}_e \frac{\partial \hat{H}_e(\bar{R})}{\partial \bar{R}_\nu} \right\} - \sum_{\nu'} \text{Tr}_e \left\{ \hat{\mu}_{1,\nu'} \frac{\partial^2 \hat{H}_e(\bar{R})}{\partial \bar{R}_\nu \partial \bar{R}_{\nu'}} \right\} - \frac{1}{2} \sum_{\nu'\nu''} \text{Tr}_e \left\{ \hat{\mu}_{2,\nu'\nu''} \frac{\partial^3 \hat{H}_e(\bar{R})}{\partial \bar{R}_\nu \partial \bar{R}_{\nu'} \partial \bar{R}_{\nu''}} \right\} + \dots \quad (35)$$

where $\hat{\rho}_e = \text{Tr}_N \{\hat{\rho}\}$, $\hat{\mu}_{1,\nu} = \text{Tr}_N \{\hat{\rho} \Delta \hat{R}_\nu\}$, and $\hat{\mu}_{2,\nu'\nu''} = \text{Tr}_N \{\hat{\rho} \Delta \hat{R}_\nu \Delta \hat{R}_{\nu'} \Delta \hat{R}_{\nu''}\}$. The first term in Eq. 35 is the Ehrenfest approximation. The higher terms account for the fact that the wave packet has some finite width, and that the mean force must include an average over the paths included within the packet. However, at this point it is important to note a fundamental distinction. There are *two* separate contributions to the total width of the wave packet. The more obvious is just the normal quantum width of the nucleus, and this contributes to $\hat{\mu}_{2,\nu'\nu''}$ and higher moments. The other contribution is due to transitions between Born-Oppenheimer surfaces. If a nucleus starts a trajectory on one particular Born-Oppenheimer energy surface, and there is some coupling to another surface, then that trajectory will split into two trajectories, one on each surface. Since the forces experienced on each surface can be different the two trajectories can deviate from one another, producing broadening of the total wave packet. The first moment ($\hat{\mu}_{1,\nu}$) contains only this contribution, but it appears in all other moments as well.

We now seek to understand the meaning of the moments. First we note that $\hat{\rho}_e$, $\hat{\mu}_{1,\nu}$ and $\hat{\mu}_{2,\nu'\nu''}$ are electronic operators (the traces have only been taken over the nuclear degrees of freedom). We can therefore take matrix elements with respect to electronic states. Suppose we have energy surfaces α characterised by a set of electronic states $|\alpha\rangle$. We then have

$$\begin{aligned} \rho_{e,\alpha\alpha} &= \langle \alpha | \hat{\rho}_e | \alpha \rangle = \int \rho_{\alpha\alpha}(\vec{R}) d\vec{R} \\ \mu_{1,\nu,\alpha\alpha} &= \langle \alpha | \hat{\mu}_{1,\nu} | \alpha \rangle = \int \rho_{\alpha\alpha}(\vec{R}) (R_\nu - \bar{R}_\nu) d\vec{R} \\ \mu_{2,\nu'\nu'',\alpha\alpha} &= \langle \alpha | \hat{\mu}_{2,\nu'\nu''} | \alpha \rangle = \int \rho_{\alpha\alpha}(\vec{R}) (R_\nu - \bar{R}_\nu)(R_{\nu'} - \bar{R}_{\nu'}) d\vec{R} \end{aligned} \quad (36)$$

where $\rho_{\alpha\alpha}(\vec{R}) = \langle \alpha \vec{R} | \hat{\rho} | \alpha \vec{R} \rangle$, and is the ionic density projected onto surface α . Thus $\rho_{e,\alpha\alpha}$ is just the probability of being on surface α . If we define the mean value of some observable \hat{Q} on surface α to be $\langle \alpha | \hat{Q} | \alpha \rangle / \rho_{e,\alpha\alpha}$ then $\mu_{1,\nu,\alpha\alpha}$ just equals the mean position of the nucleus on the surface, measured relative to the mean trajectory \bar{R}_ν , multiplied by the probability of being on that surface. Similarly, $\mu_{2,\nu'\nu'',\alpha\alpha}$ gives the width of the packet moving on surface α , multiplied by the probability of being on that surface, and thus is a measure of the quantum width of the nucleus.

Thus, in summary, the small amplitude moment expansion corrects the Ehrenfest approximation by allowing different trajectories on different energy surfaces, and by giving the nuclei a finite quantum width. To make this into a practical method we need some efficient way of evaluating the moments $\hat{\mu}_{1,\nu}$, $\hat{\mu}_{2,\nu'\nu''}$, *etc.* This is achieved by integrating their equations of motion [120]. These equations follow from the Liouville

equation (Eq. 18), and the definition of the moments. Thus we have

$$\begin{aligned}\frac{d\hat{\rho}_e}{dt} &= \frac{1}{i\hbar} [\hat{H}_e(\bar{R}), \hat{\rho}_e] - \frac{1}{i\hbar} \sum_{\nu} [\hat{F}_{\nu}, \hat{\mu}_{1,\nu}] + \dots \\ \frac{d\hat{\mu}_{1,\nu}}{dt} &= \frac{\hat{\lambda}_{1,\nu}}{M_{\nu}} + \frac{1}{i\hbar} [\hat{H}_e(\bar{R}), \hat{\mu}_{1,\nu}] + \dots \\ \frac{d\hat{\lambda}_{1,\nu}}{dt} &= \frac{1}{2} (\Delta \hat{F}_{\nu} \hat{\rho}_e + \hat{\rho}_e \Delta \hat{F}_{\nu}) - \sum_{\nu'} \frac{1}{2} (\hat{K}_{\nu\nu'} \hat{\mu}_{1,\nu'} + \hat{\mu}_{1,\nu'} \hat{K}_{\nu\nu'}) + \frac{1}{i\hbar} [\hat{H}_e(\bar{R}), \hat{\lambda}_{1,\nu}]\end{aligned}\quad (37)$$

where $\hat{F}_{\nu} = -\partial \hat{H}_e(\bar{R})/\partial \bar{R}_{\nu}$, $\Delta \hat{F}_{\nu} = \hat{F}_{\nu} - \bar{F}_{\nu}$, $\hat{K}_{\nu\nu'} = \partial^2 \hat{H}_e(\bar{R})/\partial \bar{R}_{\nu} \partial \bar{R}_{\nu'}$, $\hat{\lambda}_{1,\nu} = \text{Tr}_N \{\hat{\rho} \Delta \hat{P}_{\nu}\}$ and $\Delta \hat{P}_{\nu} = \hat{P}_{\nu} - \bar{P}_{\nu}$. We can obtain a rather straightforward interpretation of these equations by considering matrix elements of the moments with respect to the electronic states $|\alpha\rangle$, provided $\hat{H}_e(\bar{R})|\alpha\rangle = i\hbar \partial|\alpha\rangle/\partial t$. Under these conditions from Eq. 37 we obtain

$$\begin{aligned}\frac{d\rho_{e,\alpha\alpha}}{dt} &= -\frac{1}{i\hbar} \sum_{\nu\alpha'} (F_{\nu,\alpha\alpha'} \mu_{1,\nu,\alpha'\alpha} - \mu_{1,\nu,\alpha\alpha'} F_{\nu,\alpha'\alpha}) + \dots \\ \frac{d\mu_{1,\nu,\alpha\alpha}}{dt} &= \frac{\lambda_{1,\nu,\alpha\alpha}}{M_{\nu}} + \dots \\ \frac{d\lambda_{1,\nu,\alpha\alpha}}{dt} &= \Delta F_{\nu,\alpha\alpha} \rho_{e,\alpha\alpha} + \frac{1}{2} \sum_{\alpha'(\neq\alpha)} (\Delta F_{\nu,\alpha\alpha'} \rho_{e,\alpha'\alpha} + \rho_{e,\alpha\alpha'} \Delta F_{\nu,\alpha'\alpha})\end{aligned}\quad (38)$$

The first equation (for the diagonal elements of the electronic density matrix) tells us that transitions between Born-Oppenheimer surfaces are driven by force couplings between the surfaces. If we think of $\mu_{1,\nu,\alpha\alpha}$ as the position of a nucleus on the surface multiplied by the probability of being on the surface, and $\lambda_{1,\nu,\alpha\alpha}$ as the momentum of a nucleus on the surface multiplied by the probability of being on the surface (see Eq. 36), then the second equation just gives the usual relation between velocity and momentum (provided the probability of being on the surface is not changing). Finally, the third equation relates the rate of change of momentum of the nucleus on the surface to the force that it is experiencing (the diagonal force term), plus some additional corrections derived from the non-adiabatic interactions. Thus we see that the small amplitude moment expansion at lower orders is describing classical trajectories on multiple Born-Oppenheimer surfaces.

For a practical implementation of the scheme we need to truncate the infinite hierarchy of equations of motion for the moments. If we work with a fixed order of expansion for the Hamiltonian (in practice dropping cubic and higher terms in the Taylor expansion in Eq. 34), then for the highest order moments for which we have equations of motion there will be additional moments appearing in those equations for which there is no corresponding equation of motion. To produce closure we therefore need to estimate these higher moments from the lower ones already evaluated. For metallic systems, where nuclear wave packets mostly breathe without splitting, satisfactory results have been obtained [121,122] by a mean field approximation which relates $\hat{\mu}_{2,\nu\nu'}$ and other second moment operators to products of their own traces and $\hat{\rho}_e$. This procedure is a simple case of a general formalism which is currently under development. First we reconstruct an approximate density matrix from the known moments, then we perform the necessary traces with this density matrix to produce the required additional moments. This process is made much easier because of two

remarkable theorems. Consider a density matrix for which a Wigner transform has been carried out over the nuclear degrees of freedom (see Appendix B), to give $\hat{\rho}_W(\vec{R}\vec{P})$ which is an electronic operator which depends parametrically on the nuclear positions and momenta. For one nuclear degree of freedom the first theorem states [216] that

$$\int R^n P^m \hat{\rho}_W(RP) dR dP = \left(\frac{1}{2}\right)^n \sum_{l=0}^n C_l^n \text{Tr} \left\{ \hat{\rho} \hat{R}^l \hat{P}^m \hat{R}^{n-l} \right\} \quad (39)$$

which relates the moments of the Wigner matrix to those of the density matrix. The second theorem states that for quadratic Hamiltonians the moments appearing in CEID can always be written in the form given by the right-hand side of Eq. 39. In short, CEID moments are moments of the Wigner function. This has two immediate consequences. First, we do not have to worry about the order of the operators in the moments, so that we can completely characterise the moments by the powers of position and momentum. Second, since the Wigner function is a function of scalars we can approximate this function using standard techniques, rather than attempting the much more complex process of approximating functions of operators. For CEID we use harmonic oscillator eigenfunctions to expand the Wigner function (an approach which has been used in other similar contexts [217]). The final result is that the unknown moments can be expressed as a linear combination of the known, with constant coefficients[§]. An alternative approach (that has *not* been investigated with CEID) has been used in a related method [218].

To use this method with popular approximate electronic structure methods (such as Hartree-Fock or tight binding - and possibly density functional theory, though there are additional theoretical problems in this case) it is necessary to reduce the N -electron problem into a 1-electron problem (that is, an extension of Hartree-Fock theory). This is achieved by taking the N -electron equations of motion (Eq. 37) and taking a trace over all the electrons except one. This produces equations of motion for 1-electron operators. However, in those equations of motion 2-electron operators appear. To reduce the theory to a pure 1-electron theory we need to replace these 2-electron operators with suitable functions of 1-electron operators. This is based on the density matrix product used in the Hartree-Fock approximation. In matrix notation the product is $\rho(12, 1'2') \approx \rho(1, 1')\rho(2, 2') - \rho(1, 2')\rho(2, 1')$, where the numbers 1 and 2 refer to the set of indices for electrons 1 and 2 respectively. However, this equation by itself is not enough. There are two reasons: first, we need to approximate 2-electron moments as well as the electronic density matrix [120]; second, since the electron density matrix used in CEID involves a trace over multiple nuclear configurations, we need to take an appropriate average of products of single particle density matrices, even for the electron density matrix [121]. In both cases the starting point is the same, namely to write the moment (\hat{q}) we are interested in terms of the product of nuclear fluctuations (\hat{Q}) in the following way

$$\begin{aligned} \hat{q} &= \text{Tr}_N \left\{ \hat{Q} \hat{\rho} \right\} \\ &= \int Q(\vec{R}'\vec{R}) \hat{\rho}(\vec{R}\vec{R}') d\vec{R} d\vec{R}' \\ &= \int Q(\vec{R}'\vec{R}) \rho_N(\vec{R}\vec{R}') \hat{\rho}_e(\vec{R}\vec{R}') d\vec{R} d\vec{R}' \end{aligned} \quad (40)$$

[§] There are also additional correction terms that appear in the equations of motion for the moments because of the truncation. These emerge by deriving the equations of motion from an effective Lagrangian. This work will be described in a forthcoming paper.

where $\hat{\rho}(\vec{R}\vec{R}') = \langle \vec{R} | \hat{\rho} | \vec{R}' \rangle$, $\rho_N(\vec{R}\vec{R}') = \text{Tr}_e \{ \hat{\rho}(\vec{R}\vec{R}') \}$ and $\hat{\rho}_e(\vec{R}\vec{R}') \times \rho_N(\vec{R}\vec{R}') = \hat{\rho}(\vec{R}\vec{R}')$. The operator $\hat{\rho}_e(\vec{R}\vec{R}')$ is an electronic density matrix to which we apply the Hartree-Fock approximation. To evaluate the integrals over nuclear coordinates we need to make an approximation for the \vec{R} dependence of $\hat{\rho}_e(\vec{R}\vec{R}')$. We make a Taylor expansion in powers of $\Delta\vec{R}$ about $\hat{\rho}_e(\vec{R}\vec{R})$, which corresponds to weak dynamic coupling between the electrons and nuclei. For details see references [120, 121]. Here we briefly consider the the result of the above procedure for the electronic density matrix:

$$\begin{aligned} \rho_e^{(2)}(12; 1'2') \approx & \rho_e^{(1)}(11')\rho_e^{(1)}(22') - \rho_e^{(1)}(12')\rho_e^{(1)}(21') + \\ & \sum_{\nu\nu'} D_{\nu\nu'}^{RR} \left(\mu_{1,\nu'}^{(1)}(11')\mu_{1,\nu}^{(1)}(22') - \mu_{1,\nu'}^{(1)}(12')\mu_{1,\nu}^{(1)}(21') \right) + \dots \end{aligned} \quad (41)$$

where $\rho_e^{(2)}(12; 1'2')$, $\rho_e^{(1)}(11')$ and $\mu_{1,\nu'}^{(1)}(11')$ are the matrix representations of the two-electron density matrix, the one electron density matrix and the one electron first moment respectively. The matrix $D_{\nu\nu'}^{RR}$ is the inverse of $C_{\nu\nu'}^{RR} = \text{Tr}_e \{ \hat{\mu}_{2,\nu\nu'} \}$. We see that the density matrix is not quite idempotent even for noninteracting electrons, which is because there are electron-ion correlations and a dynamical response of the electrons to nuclear fluctuations. This response, described by the second term, screens the ion-ion interactions. The resultant dynamical stiffness corrections are essential for getting the correct phonon structure and inelastic electron-phonon spectrum [121, 122].

Historically, CEID was developed to allow electric current induced heating in nanoscale devices to be modelled. Therefore, open boundaries have been a consideration from the beginning, and have now been implemented in two ways. The first starts from Eqs. 33 and 37 given above [123, 219]. To produce a finite system with open boundaries we consider our system as being embedded in an infinite environment, and apply our equations of motion to the infinite combined system. Clearly we cannot explicitly evolve the electron density matrix and the moments for an infinite system, so we make use of the fact that we can write down analytic solutions for the evolution of the electron density matrix and the moments provided that the Hamiltonian does not vary with time. This allows us to write down closed form solutions for the environment which we then couple to the explicit time evolution of the system in which we are interested. To produce numerically stable solutions it is found necessary to introduce a small amount of damping into the environment. For details see references [123, 219]. The second scheme, which is currently under development, achieves numerical simplifications at the expense of additional approximations.

So how does this method compare with others? We have already discussed its relationship to the Ehrenfest approximation, and clearly it introduces those essential features to the theory that allow a proper transfer of energy between electrons and nuclei. From Eq. 38 we can see some correspondence with surface hopping (see section 3.3.2), but with the important difference that different trajectories are able to remain coherent with one another as they are treated simultaneously rather than independently. A further important feature is that this method reproduces results of Fermi's golden rule for the exchange of energy between electrons and nuclei provided that the second moment is retained [121]. More broadly, the strengths of CEID are that it is not perturbative, it does not invoke the notion of phonons and is inherently anharmonic, it avoids classical interpretations of quantum transitions,

and it in principle contains the mutual screening of the three interactions (electron-electron, electron-nucleus, nucleus-nucleus), while retaining the conceptual framework of molecular dynamics.

CEID is still a rather young method, so a limited range of results has so far been produced. It has been applied to Joule heating in atomic wires [120], in which case it was found that the first moments ($\hat{\mu}_{1,\nu}$ and $\hat{\lambda}_{1,\nu}$) were essential for producing the correct heating. The second moments (which involve $\Delta\hat{R}_\nu\Delta\hat{R}_{\nu'}$, $\Delta\hat{P}_\nu\Delta\hat{R}_{\nu'}$ and $\Delta\hat{P}_\nu\Delta\hat{P}_{\nu'}$) are needed to describe the change in electrical resistance due to increased nuclear vibrations [121, 122]. Once these were included, it was possible to reproduce the spectral signature of the inelastic scattering of electrons by nuclei.

4. Conclusion and future directions

Above we have surveyed some of the phenomena resulting from, and the current state of theories for understanding, the exchange of energy between electrons and nuclei. Accurate modelling of the phenomena is a hard problem because of its intrinsically many-body and correlated nature. As a consequence, all the theories are in need of further development, as has been indicated in the text. As the different theories have different attributes (some are perturbative, others are based on molecular dynamics, and so on), they can naturally be applied to different problems. So there is a need for development on more than one front.

The biggest advance is probably going to be in the range of problems to be addressed using these techniques. There are now standard phenomena that are studied or used to test novel methods, such as heating in nanocontacts, or photodissociation, but they are limited in scope. Non-equilibrium phenomena, by contrast, are ubiquitous. Certainly the modelling of molecular electronic devices and biological molecules associated with non-equilibrium electrons (such as DNA and retinal) have already begun to be investigated, and their importance must surely increase. Other problems that should benefit from new methods include the evolution of radiation damage and inelastic tunneling spectroscopy carried out with STMs.

Acknowledgments

C.G.S. is grateful to CONICET for support. DRB is supported by the Royal Society. This study was partly performed through Special Coordination Funds for Promoting Science and Technology from the MEXT, Japan. APH is supported by the IRC in Nanotechnology. HN would like to thank Th. Martin and M. Brandbyge for illuminating and enriching discussions about non-equilibrium Green's functions. Continued research on CEID is being supported by the EPSRC, grant numbers EP/C524381/1, EP/C006739/1 and EP/C524403/1.

Appendix A. Electron-phonon Hamiltonians

There are two common approaches to building Hamiltonians that couple electronic and nuclear dynamics (adiabatic states and static lattice states). Even though they have been shown to give formally the same answers in lowest order perturbation theory [220], there may be practical reasons for choosing one over the other. We summarise the basic equations for each case below. Occasionally it is useful to use the

diabatic representation of the electronic states. This is obtained from the adiabatic representation discussed below by a unitary transform that makes the nuclear kinetic energy operator diagonal.

Appendix A.1. Adiabatic states

The Hamiltonian for a system of electrons and nuclei we write as $\hat{H} = \hat{T}_N + \hat{H}_e(\hat{R})$, where \hat{T}_N is the nuclear kinetic energy, $\hat{H}_e(\hat{R})$ is the Hamiltonian for electrons in the field of the nuclei, and \hat{R} is the position operator for all the nuclei. In the Born-Oppenheimer (adiabatic) separation, we assume that we can neglect the nuclear kinetic energy to begin with. This then produces the following Schrödinger equation for the electrons in the field of the nuclei

$$\hat{H}_e(\vec{R})\Phi_n(\vec{R}) = E_n(\vec{R})\Phi_n(\vec{R}) \quad (\text{A.1})$$

Note that nuclear positions are now represented by numbers \vec{R} , and not operators. The subscript n indexes the Born-Oppenheimer surfaces. Now that we have a set of electronic states $\Phi_n(\vec{R})$, adiabatic nuclear states χ_{nN} can be generated by treating $E_n(\vec{R})$ as an effective potential for the nuclei, giving

$$(\hat{T}_N + E_n(\vec{R}))\chi_{nN} = U_{nN}\chi_{nN} \quad (\text{A.2})$$

where the subscript N indexes the allowed nuclear states, and U_{nN} is the total adiabatic energy (electrons and nuclei). Equipped with these states, we can now use Fermi's Golden Rule to find transition rates between the product states $\Psi_{nN} = \chi_{nN}\Phi_n$, giving the matrix elements $M_{nNn'N'} = \int d\vec{R}d\vec{r}\Psi_{nN}^*\hat{H}\Psi_{n'N'}$

$$M_{nNn'N'} = U_{nN}\delta_{nn'}\delta_{NN'} + \int d\vec{R}\chi_{nN}^*\chi_{n'N'} \left[\int d\vec{r}\Phi_n^*\hat{T}_N\Phi_{n'} + \sum_{\nu} \frac{\hat{P}_{\nu}\chi_{n'N'}}{M_{\nu}\chi_{n'N'}} \int d\vec{r}\Phi_n^*\hat{P}_{\nu}\Phi_{n'} \right] \quad (\text{A.3})$$

where \vec{r} is the set of electronic positions, the subscript ν indexes the individual nuclear coordinates, \hat{P}_{ν} is the corresponding nuclear momentum operator, and M_{ν} the nuclear mass. The energies appearing in Fermi's Golden Rule are U_{nN} . If we assume that the energy surfaces on which the nuclei are moving are harmonic, then the nuclear wave functions are the simple harmonic oscillator wave functions characterised by a frequency, a mass, and an equilibrium position. Further, the energies will satisfy

$$U_{nN} = E_n(\vec{R}_{n,0}) + \sum_{\alpha} \left(n_{N\alpha} + \frac{1}{2} \right) \hbar\omega_{n,\alpha} \quad (\text{A.4})$$

where $\vec{R}_{n,0}$ corresponds to the equilibrium positions of nuclei on surface n , and α is an index running over the normal modes which have angular frequencies $\omega_{n,\alpha}$ and occupancies $n_{N\alpha}$. The surface dependence of the vibrational frequencies is often neglected, that is $\omega_{n,\alpha} = \omega_{0,\alpha}$.

Appendix A.2. Static lattice states

This approach starts with the following partitioning of the Hamiltonian:

$$\begin{aligned} \hat{H} &= \hat{T}_N + \hat{H}_e(\vec{R}) \\ &= [\hat{T}_N + E_0(\vec{R}) - E_0(\vec{R}_0)] + \hat{H}_e(\vec{R}_0) + [(\hat{H}_e(\vec{R}) - E_0(\vec{R})) - (\hat{H}_e(\vec{R}_0) - E_0(\vec{R}_0))] \\ &= \hat{H}_N + \hat{H}_e(\vec{R}_0) + \hat{H}_{eN} \end{aligned} \quad (\text{A.5})$$

where \vec{R}_0 is the equilibrium positions of the nuclei in the ground state, and $E_0(\vec{R})$ is the ground state Born-Oppenheimer energy surface. The electronic states Φ_n are given by

$$\hat{H}_e(\vec{R}_0)\Phi_n = E_n\Phi_n \quad (\text{A.6})$$

There are two important limits in which we can define the states of the nuclear subsystem. When the electron-nuclear coupling \hat{H}_{eN} is *always* weak then the reference nuclear wavefunctions χ_N are found from

$$\hat{H}_N\chi_N = W_N\chi_N \quad (\text{A.7})$$

Fermi's Golden Rule can then be used to find transition rates between the product states $\Psi_{nN} = \chi_N\Phi_n$, giving the matrix elements

$$M_{nNn'N'} = (E_n + W_N)\delta_{NN'}\delta_{nn'} + \int d\vec{R}d\vec{r}\chi_N^*\Phi_n^*\hat{H}_{eN}\chi_{N'}\Phi_{n'} \quad (\text{A.8})$$

In the limit of small ionic displacements we can use a linear approximation for the interaction Hamiltonian, which is $\hat{H}_{eN} \approx (\vec{R} - \vec{R}_0) \cdot \vec{\nabla}\hat{H}_e(\vec{R}_0)$, where we have used the definition of the fixed sites, namely $\vec{\nabla}E_0(\vec{R}_0) = 0$. Matrix elements of this Hamiltonian have the form

$$\int d\vec{R}d\vec{r}\chi_N^*\Phi_n^*\hat{H}_{eN}\chi_{N'}\Phi_{n'} = \int d\vec{R}\chi_N^*(\vec{R} - \vec{R}_0)\chi_{N'} \cdot \int d\vec{r}\Phi_n^*\vec{\nabla}\hat{H}_e(\vec{R}_0)\Phi_{n'} \quad (\text{A.9})$$

The energies appearing in Fermi's Golden Rule are $U_{nN} = E_n + W_N$. If the ground state Born-Oppenheimer energy surface is harmonic, then the nuclear wave functions will be simple harmonic oscillator wave functions centred about the ground state equilibrium positions. The nuclear energies will satisfy

$$W_N = \sum_{\alpha} \left(n_{N\alpha} + \frac{1}{2} \right) \hbar\omega_{\alpha} \quad (\text{A.10})$$

where α is an index running over the normal modes which have angular frequencies ω_{α} and occupancies $n_{N\alpha}$.

The second case corresponds to the electron-nuclear coupling being weak only *between* energy surfaces, but strong on a surface. In this case the minimum energy configurations of different adiabatic energy surfaces are displaced significantly from one another. If we treat the electron-nuclear coupling \hat{H}_{eN} with the linear approximation we then partition $\hat{F} = -\vec{\nabla}\hat{H}_e(\vec{R}_0)$ into diagonal (\hat{F}_D) and off-diagonal (\hat{F}_{OD}) terms, where $\int d\vec{r}\Phi_n^*\hat{F}_D\Phi_{n'} = \delta_{nn'} \int d\vec{r}\Phi_n^*\hat{F}\Phi_{n'}$ and $\int d\vec{r}\Phi_n^*\hat{F}_{OD}\Phi_{n'} = (1 - \delta_{nn'}) \int d\vec{r}\Phi_n^*\hat{F}\Phi_{n'}$. The diagonal Schrödinger equation then becomes $(\hat{H}_N + \hat{H}_e(\vec{R}_0) - \hat{F}_D \cdot (\vec{R} - \vec{R}_0))\Phi_n\tilde{\chi}_{nN} = \tilde{U}_{nN}\Phi_n\tilde{\chi}_{nN}$, where now the nuclear states $\tilde{\chi}_{nN}$ depend on electronic state. If we make the Harmonic approximation for the nuclear Hamiltonian $\hat{H}_N = \hat{T}_N + \frac{1}{2}\vec{u} \cdot \mathbf{K} \cdot \vec{u}$, where \mathbf{K} is the matrix of spring constants and $\vec{u} = \vec{R} - \vec{R}_0$ is the displacement of the nuclei relative to the reference positions, then we get

$$\left(\hat{T}_N + \frac{1}{2}(\vec{u} - \vec{u}_n) \cdot \mathbf{K} \cdot (\vec{u} - \vec{u}_n) + E_n - \frac{1}{2}\vec{u}_n \cdot \mathbf{K} \cdot \vec{u}_n \right) \tilde{\chi}_{nN} = \tilde{U}_{nN}\tilde{\chi}_{nN} \quad (\text{A.11})$$

where the displacement \vec{u}_n is defined by $\mathbf{K} \cdot \vec{u}_n = \int \Phi_n^*\hat{F}_D\Phi_n d\vec{r}$. This is just the equation of motion for a shifted oscillator whose potential minimum is at \vec{u}_n , and whose energy at the minimum is $E_{n,0} = E_n - \frac{1}{2}\vec{u}_n \cdot \mathbf{K} \cdot \vec{u}_n$. The oscillator wavefunctions

are just given by $\tilde{\chi}_{nN}(\vec{u}) = \chi_{nN}(\vec{u} - \vec{u}_n)$. The energies appearing in Fermi's Golden rule are now

$$\tilde{U}_{nN} = E_{n,0} + \sum_{\alpha} \left(n_{N\alpha} + \frac{1}{2} \right) \hbar\omega_{\alpha} \quad (\text{A.12})$$

and the matrix elements are

$$M_{nNn'N'} = -(1 - \delta_{nn'}) \int \Phi_n^* \hat{F} \Phi_{n'} d\vec{r} \cdot \int \chi_N^*(\vec{u} - \vec{u}_n) \vec{u} \chi_{N'}(\vec{u} - \vec{u}_{n'}) d\vec{R} \quad (\text{A.13})$$

Appendix B. The Wigner transform

CEID is formulated in terms of the density matrix, which is then characterised by moments of the position and momentum fluctuations of the ions. These moments are reminiscent of moments of classical phase space distributions, and so it is natural to seek a formal connection. This can be achieved by appealing to the Wigner matrix [119, 216, 221] which is constructed by applying a transformation to the density matrix $\hat{\rho}$ which is a function of both electronic and nuclear degrees of freedom. Let us use a real space representation ($|\vec{X}\rangle$) of the N nuclear degrees of freedom, and leave the electronic ones abstract, giving $\hat{\rho}(\vec{X}, \vec{X}') = \langle \vec{X} | \hat{\rho} | \vec{X}' \rangle$. If we make the following linear combinations, $\vec{R} = (\vec{X} + \vec{X}')/2$ and $\vec{S} = \vec{X} - \vec{X}'$, and carry out a Fourier transformation with respect to \vec{S} , we get the Wigner matrix

$$\hat{\rho}_W(\vec{R}, \vec{P}) = \frac{1}{h^N} \int \hat{\rho}(\vec{R} + \frac{1}{2}\vec{S}, \vec{R} - \frac{1}{2}\vec{S}) \exp(\vec{S} \cdot \vec{P}/i\hbar) d\vec{S} \quad (\text{B.1})$$

The connection between this function and a classical phase space distribution can be seen from the following

- (i) If we integrate $\hat{\rho}_W(\vec{R}, \vec{P})$ over \vec{P} , we get back the quantum spatial distribution function $\hat{\rho}(\vec{R}, \vec{R})$.
- (ii) If we integrate $\hat{\rho}_W(\vec{R}, \vec{P})$ over \vec{R} , we get the quantum momentum distribution function $\hat{\rho}(\vec{P}, \vec{P})$.
- (iii) It has an equation of motion similar to that of the classical Liouville equation in the classical limit defined by $\hbar \rightarrow 0$, which also corresponds to heavy nuclei [222]

$$\begin{aligned} \frac{\partial \hat{\rho}_W(\vec{R}, \vec{P})}{\partial t} &= \frac{1}{i\hbar} \left[\hat{H}_e(\vec{R}), \hat{\rho}_W(\vec{R}, \vec{P}) \right] \\ &\quad - \frac{\vec{P}}{M} \cdot \frac{\partial \hat{\rho}_W(\vec{R}, \vec{P})}{\partial \vec{R}} + \frac{1}{2} \left\{ \frac{\partial \hat{H}_e(\vec{R})}{\partial \vec{R}} \cdot \frac{\partial \hat{\rho}_W(\vec{R}, \vec{P})}{\partial \vec{P}} + \frac{\partial \hat{\rho}_W(\vec{R}, \vec{P})}{\partial \vec{R}} \cdot \frac{\partial \hat{H}_e(\vec{R})}{\partial \vec{R}} \right\} \\ &\quad + \mathcal{O}(\hbar) \end{aligned}$$

Appendix C. Equilibrium and non-equilibrium Green's functions

In this appendix we give the definition of the different Green's functions, we also briefly introduce the technique of the Keldysh time-contour applied to non-equilibrium conditions, and derive the corresponding Green's functions and self-energies in the presence of interactions.

Appendix C.1. General definitions

Let us consider two operators A and B . The retarded r , advanced a , time-ordered t and antichronological time-ordered \tilde{t} Green's function with real time arguments are defined as

$$\begin{aligned} G_{A;B}^r(t, t') &= -i\theta(t - t')\langle [A(t), B(t')]_{\pm} \rangle, \\ G_{A;B}^a(t, t') &= i\theta(t' - t)\langle [A(t), B(t')]_{\pm} \rangle, \\ G_{A;B}^t(t, t') &= -i\langle T_t (A(t)B(t')) \rangle = -i\theta(t - t')\langle A(t)B(t') \rangle \pm i\theta(t' - t)\langle B(t')A(t) \rangle, \\ G_{A;B}^{\tilde{t}}(t, t') &= -i\langle T_{\tilde{t}} (A(t)B(t')) \rangle = -i\theta(t' - t)\langle A(t)B(t') \rangle \pm i\theta(t - t')\langle B(t')A(t) \rangle \end{aligned} \quad (\text{C.1})$$

The average $\langle \dots \rangle$ is taken over the many-body ground state and $A(t)$ is given in the Heisenberg representation. The $+$ sign applies when the operators A and B satisfy fermion anticommutation relations, and the $-$ sign applies if A and B are boson operators. For some applications it is useful to consider Green's functions without time ordering. They are the so-called greater $>$ and lesser $<$ Green's functions:

$$G_{A;B}^>(t, t') = -i\langle A(t)B(t') \rangle \text{ and } G_{A;B}^<(t, t') = \pm i\langle B(t')A(t) \rangle,$$

with the same sign convention as above. All the other Green's functions can be defined in terms of these two Green's functions as

$$\begin{aligned} G_{A;B}^r(t, t') &= \theta(t - t')[G_{A;B}^>(t, t') - G_{A;B}^<(t, t')], \\ G_{A;B}^a(t, t') &= \theta(t' - t)[G_{A;B}^<(t, t') - G_{A;B}^>(t, t')], \\ G_{A;B}^t(t, t') &= \theta(t - t')G_{A;B}^>(t, t') + \theta(t' - t)G_{A;B}^<(t, t'). \end{aligned} \quad (\text{C.2})$$

At (thermal) equilibrium or in a stationary state regime, the Green's functions depend on the time difference only (*i.e.* $G_{A;B}^x(t, t') = G_{A;B}^x(t - t')$), and their Fourier transform is dependent on only one energy argument $G^x(\omega)$. The advanced and retarded Green's functions $G^{a,r}(\omega)$ contain information about the spectral density of the system, while the lesser and greater Green's functions $G^{<,>}(\omega)$ contain information about both the spectral density and the occupancy of the system at or out of equilibrium.

Appendix C.2. Non-equilibrium conditions and time loop contour

Here we briefly explain the principles of non-equilibrium Green's function [84, 85]. Consider a many particle system with interactions and/or with a coupling to an external driving force (external field). We want to study the system by reducing its mathematical description to the calculation of a perturbation series, with the hope that later on we can resum some (if not all) the contributions, as is usually done in many-body statistical physics [99, 223, 224]. Therefore, we start from the non-interacting ground state at the infinitely remote past (where there are no interactions) and the interaction V is turned on adiabatically. Then the different Green's functions are calculated by going to the interaction picture and evaluating the terms of the perturbation expansion series with Wick's theorem. This theorem applies to a time-ordered average with respect to a Hamiltonian that is quadratic in creation/annihilation operators (for example, a non-interacting Hamiltonian). According to Wick's theorem, the average of any product of operators can be found by forming all pairs of operators and replacing these by their average.

For a non-equilibrium (interacting) system, the ground state in the future is not known *a priori*, and we are left with average products which are only partially time

ordered. The Keldysh recipe is to introduce a time contour along which the operators can be ordered. The time contour C_K contains two branches, the upper (+) and the lower (−) branch. On the upper branch, time starts in the infinitely remote past and evolves forwards, then at the turning point (which can be placed at any arbitrary time), one passes onto the lower branch where the system evolves backwards in time back to the initially non-interacting starting point at $t = -\infty$. Then any expectation value of products of operator reduces to $\langle \phi_0 | T_{C_K} (\hat{A}(t)\hat{B}(t') \dots S_{C_K}) | \phi_0 \rangle$ where $\langle \phi_0 | \dots | \phi_0 \rangle$ is the average over the non-interacting ground state. The operators are given in the interaction picture, *i.e.* $\hat{A}(t) = e^{iH_0 t/\hbar} A e^{-iH_0 t/\hbar}$. S_{C_K} is the generalization of the time evolution operator (Eq. 10) on the time loop contour $S_{C_K} = T_{C_K} \left(\exp\{-i/\hbar \int_{C_K} d\tau \hat{V}(\tau)\} \right)$ where T_{C_K} is the time-ordering operator on the contour C_K and $\int_{C_K} dt$ implies integration over C_K . With these definitions, any time ordered product can be calculated using the usual rules of many-body perturbation theory (Feynman diagrammatic expansion, Wick's theorem, *etc.*) [99, 223, 224]. The Keldysh recipe is equivalent to reducing the problem to the calculation of averages over the non-interacting ground state, which is a great achievement because such averages can be calculated exactly in a lot of cases [100]. However, there is a price to pay for that: now we have to work with four different Green's functions defined by the position of the two times (t, t') on C_K . When the two times (t, t') are on the same branch, the time ordering T_{C_K} is equivalent to the standard time ordering: forward time ordering on the upper branch and backward time (or anti-time) ordering on the lower branch. When (t, t') are on different branches, the time ordering is such that any time on the lower branch is always later on the time loop contour C_K than any time on the upper branch.

The electron Green's function defined from the fermion operator Ψ (with the definitions in section Appendix C.1: $A = \Psi$ and $B = \Psi^\dagger$) $G(t, t') = -i\langle T_{C_K} (\Psi(t)\Psi^\dagger(t')) \rangle$ has four Keldysh components on C_K : for (t, t') on the upper branch (+) $G(t, t') = -i\langle T_{C_K} (\Psi(t_+)\Psi^\dagger(t'_+)) \rangle = G^t(t, t')$; for (t, t') on the lower branch (−) $G(t, t') = -i\langle T_{C_K} (\Psi(t_-)\Psi^\dagger(t'_-)) \rangle = G^{\tilde{t}}(t, t')$; for t on the (+) branch and t' on the (−) branch $G(t, t') = -i\langle T_{C_K} (\Psi(t_+)\Psi^\dagger(t'_-)) \rangle = G^<(t, t')$; and finally for t on the (−) branch and t' on the (+) branch $G(t, t') = -i\langle T_{C_K} (\Psi(t_-)\Psi^\dagger(t'_+)) \rangle = G^>(t, t')$. However these Green's functions are not completely independent. They satisfy the following relations: $G^t + G^{\tilde{t}} = G^< + G^>$ and $G^r - G^a = G^> - G^<$ (with the retarded and advanced Green's functions defined as in section Appendix C.1 with $A = \Psi$ and $B = \Psi^\dagger$). The self-energy Σ , associated with the interaction V for example, also has four components on the contour C_K .

It can be shown that the Green's function in the presence of interaction G is related to the Green's function in the absence of interaction G_0 via the usual Dyson equation $G(t, t') = G_0(t, t') + \int_{C_K} dt_1 dt_2 G_0(t, t_1) \Sigma(t_1, t_2) G(t_2, t')$ where the time integrals are taken over C_K . The Dyson equation can then be re-expressed using only integrals over the real-time axis by introducing the different components of G and Σ on the contour C_K . By using the relation between the different Green's functions, we finally obtain a Dyson-like equation for the advanced and retarded (non-equilibrium) Green's functions: $G^{r,a} = G_0^{r,a} + G_0^{r,a} \Sigma^{r,a} G^{r,a}$ and another kinetic equation for the (non-equilibrium) lesser and greater Green's functions: $G^{<,>} = (1 + G^r \Sigma^r) G_0^{<,>} (1 + \Sigma^a G^a) + G^r \Sigma^{<,>} G^a$. In these equations, the products $G\Sigma$ or ΣG imply time integration over the real axis, *i.e.* $\int_{-\infty}^{+\infty} dt$. Similar results can be derived

for the phonon Green's functions (*i.e.* when A and B are phonon field operators).

In principle, we can now calculate exactly the non-equilibrium properties of a many-body interacting system by determining self-consistently the different Green's functions and self-energies (knowing that the self-energies are functionals of the different Green's functions themselves).

Appendix C.3. Electron and phonon Green's functions

Appendix C.3.1. Non-interacting systems For quadratic Hamiltonians (*i.e.* non-interacting particles), we can calculate exactly the different Green's functions. Let us start with electrons and consider the electronic Hamiltonian $H_0 = \sum_n \epsilon_n c_n^\dagger c_n$. The operator c_n^\dagger (c_n) creates (annihilates) an electron in the n -th electronic state with energy ϵ_n ; n labels either the eigenstates of a finite size system or the k -states of a (1,2,3)-dimensional periodic system. With the definitions given in the previous sections and taking $A = c_n$ and $B = A^\dagger$, we find the following Green's functions in the energy representation:

$$G_0^{r,a}(\omega) = \frac{1}{\omega - \epsilon_n \pm i\eta} \text{ with } \eta \rightarrow 0^+,$$

$$G_0^<(\omega) = 2\pi i \langle c_n^\dagger c_n \rangle \delta(\omega - \epsilon_n), \quad G_0^>(\omega) = -2\pi i (1 - \langle c_n^\dagger c_n \rangle) \delta(\omega - \epsilon_n). \quad (\text{C.3})$$

The average $\langle c_n^\dagger c_n \rangle$ gives the occupation number of the state n , and in the thermodynamic limit it is given by the Fermi-Dirac distribution $f(\epsilon_n) = 1/(e^{\beta(\epsilon_n - \mu)} + 1)$ where μ is chemical potential and $\beta = 1/k_B T$.

For phonons with a quadratic Hamiltonian $H_0 = \sum_\lambda \hbar\omega_\lambda (a_\lambda^\dagger a_\lambda + 1/2)$ where a_λ^\dagger (a_λ) creates (annihilates) a quantum of energy $\hbar\omega_\lambda$, we find the following Green's functions (denoted by the letter D) defined from $A = a_\lambda^\dagger + a_\lambda$ and $B = A^\dagger$:

$$D_0^{r,a}(\omega) = \frac{1}{\omega - \omega_\lambda \pm i\eta} - \frac{1}{\omega + \omega_\lambda \pm i\eta} \text{ with } \eta \rightarrow 0^+,$$

$$D_0^{<,>}(\omega) = -2\pi i \{ \langle n_\lambda \rangle \delta(\omega \mp \omega_\lambda) + (1 + \langle n_\lambda \rangle) \delta(\omega \pm \omega_\lambda) \}, \quad (\text{C.4})$$

where $n_\lambda = a_\lambda^\dagger a_\lambda$. In the thermodynamic limit, $\langle n_\lambda \rangle$ is given by the Bose-Einstein distribution $N(\omega) = 1/(e^{\beta\omega} - 1)$.

Appendix C.3.2. Coupling to reservoirs If the (finite size) system of interest is connected to M other subsystems (generally much larger) which act as either thermal reservoirs or particle reservoirs, then we can calculate the full Green's function of the connected primary system (or central region) from the Green's function of the isolated parts of the system. This is done by solving the Dyson equation and the quantum kinetic equation for the non-equilibrium Green's functions. As an example, we consider that the coupling to the M subsystems is given by the Hamiltonian matrices V_α corresponding to electron hopping between the primary system and the M other subsystems. When neglecting the interactions between particles, the self-energies $\Sigma^{x=(r,a,<,>)}$ entering the Dyson equations for the electron Green's functions G^x of the central region (coupled to the M reservoirs) are $\Sigma^x = \sum_{\alpha=1}^M \Sigma_\alpha^x$ where $\Sigma_\alpha^x(\omega) = V_\alpha g_{\alpha\alpha}^x(\omega) V_\alpha$ and $g_{\alpha\alpha}^x$ is the corresponding Green's function of the isolated α -th subsystem (Eq. C.3).

For a central region consisting only of phonon modes λ coupled to another phonon bath (set of phonon of frequency ω_β) via some coupling constants U_β , one can derive the full phonon Green's function of the central region as $D^{r,a} = [D_0^{r,a-1} - \Pi_\lambda^{r,a}]^{-1}$

where $D_0^{r,a}$ is the bare phonon Green's function given in Eq. C.4 and the self-energy $\Pi_\lambda^{r,a}$ arises from the coupling of the modes λ to the modes β . In the simplest case, $\Pi_\lambda^{r,a}$ can be approximated by $\Pi_\lambda^{r,a}(\omega) \propto i \sum_\beta |U_\beta|^2 \delta(\omega - \omega_\beta)$ [225].

In more realistic systems, the central region needs to be described by a Hamiltonian that also includes interaction between electrons or between electrons and phonons. In the next section, the case of electron-phonon interaction is considered in detail.

Appendix C.3.3. Self-energies for electron-phonon interaction A general form for the linear electron-phonon (e-ph) interaction Hamiltonian is as follows: $H_{\text{eph}} = \sum_{\lambda,n,m} \gamma_{\lambda nm} (a_\lambda^\dagger + a_\lambda) c_n^\dagger c_m$ where $\gamma_{\lambda nm}$ are the matrix elements of the e-ph coupling matrix $\bar{\gamma}_\lambda$. For such an interaction, one needs to include another contribution Σ_{eph}^x in the electron self-energies $\Sigma^x = \sum_{\alpha=1}^M \Sigma_\alpha^x$. Similarly, one has to include the contribution due to the e-ph interaction in the phonon self-energies Π_λ^x .

As mentioned in section 3.2.3, within the self-consistent Born approximation, the lowest-order perturbation expansion for the interaction is used to determine the self-energies and then the non-interacting Green's functions are substituted by the full Green's functions of the system. As an example, the contribution from the Fock-diagrams to the electron self-energy is: $\Sigma^F(t, t') \propto i \sum_\lambda D(t, t') \bar{\gamma}_\lambda G(t, t') \bar{\gamma}_\lambda$ (t and t' being on the contour C_K). Using Langreth's rules for products of operators on C_K [226], one gets the different contributions to the self-energy in the following form: $\Sigma_{\text{eph}}^{xy}(\omega) \propto i \int d\omega' D^x(\omega - \omega') \bar{\gamma}_\lambda G^y(\omega') \bar{\gamma}_\lambda$, where $x, y = (r, a, <, >)$. For example, the retarded Fock part of the electron self-energy is given by: $\Sigma_{\text{eph}}^{F,r} = \Sigma_{\text{eph}}^{r<} + \Sigma_{\text{eph}}^{rr} + \Sigma_{\text{eph}}^{<r}$. The exact expressions for the different self-energies can be found in Refs. [103, 104, 115, 116, 227]. The contribution to the phonon self-energies Π_λ^x can be calculated to second order in the e-ph coupling by considering diagrams for electron-hole excitations. The polarisation Π_λ can be obtained from $\Pi_\lambda(t, t') \propto i \text{Tr}\{\bar{\gamma}_\lambda G(t, t') \bar{\gamma}_\lambda G(t', t)\}$ where the trace runs over the electron states n . Once again, one has to use Langreth's rules to obtain the different contributions $\Pi_\lambda^{a,r,<,>}(\omega)$ which can be found in Refs. [106, 107, 109, 115]. And finally, we solve the problem by calculating the different electron and phonon full Green's functions $G^{a,r,<,>}(\omega)$ and $D_\lambda^{a,r,<,>}(\omega)$ from the coupled Dyson and quantum kinetic equations, with the self-energies being functionals in the following form: $\Sigma_{\text{eph}}^{a,r,<,>}(\omega) = \Sigma[\{G^x(\omega)\}, \{D^x(\omega)\}]$ and $\Pi_\lambda^{a,r,<,>}(\omega) = \Pi[\{G^x(\omega)\}, \{D^x(\omega)\}]$.

References

- [1] Joule J 1845 *Phil. Mag.* **27** 205
- [2] Ziman J M 1960 *Electrons and phonons* (OUP)
- [3] Muller C J, van Ruitenbeek J M and de Jongh L J 1992 *Phys. Rev. Lett.* **69** 140–143
- [4] van den Brom H E, Yanson A I and van Ruitenbeek J M 1998 *Physica B* **252** 69–75
- [5] Smit R H M, Untiedt C and van Ruitenbeek J M 2004 *Nanotechnology* **15** S472–S478
- [6] Ralls K S, Ralphs D C and Buhrman R A 1989 *Phys. Rev. B* **40**(17) 11561–11570
- [7] Holweg P A M, Caro J, Verbruggen A H and Radelaar S 1992 *Phys. Rev. B* **45**(16) 9311–9319
- [8] Todorov T N 1998 *Phil. Mag. B* **77**(4) 965–973
- [9] Stoneham A M 1981 *Rep. Prog. Phys., Vol. 44, 1981*. **44**(1) 37–44
- [10] Stoneham A M 2001 *Theory of Defects in Solids: Electronic Structure of Defects in Insulators and Semiconductors* (Oxford University Press)
- [11] Boer K W 2002 *Survey of semiconductor physics* (Wiley Interscience)

- [12] Standley K J and Vaughan R A 1969 *Electron spin relaxation phenomena in solids* (Hilger, London)
- [13] Stevens K W H 1967 *Rep. Prog. Phys.* **30**(1) 189–226
- [14] Brya W J and Wagner P E 1967 *Phys. Rev.* **157**(2) 400–410
- [15] Gundogdu K, Hall K C, Koerperick E J, Pryor C E, Flatte M E, Boggess T F, Shchekin O B and Deppe D G 2005 *App. Phys. Lett.* **86**(11) 113111
- [16] Buyanova I A, Rudko G Y, Chen W M, Kyanuma K, Murayama A, Oka Y, Toropov A A, Sorokin S V and Ivanov S V 2005 *Phys. Rev. B* **71**(16) 165203
- [17] Lu C, Cheng J L and Wu M W 2005 *Phys. Rev. B* **71**(7) 075308
- [18] Haynes J R 1966 *Phys. Rev. Lett.* **17**(16) 860–862
- [19] Choyke W J and Patrick L 1962 *Phys. Rev.* **127**(6) 1868–1877
- [20] Gilleo M A, Bailey P T and Hill D E 1968 *Phys. Rev.* **174**(3) 898–905
- [21] Wohlgemant M, Tandon K, Mazumdar S, Ramasesha S and Vardeny Z V 2001 *Nature* **409** 494–497
- [22] Feldmann J, Peter G, Gobel E O, Dawson P, Moore K, Foxon C and Elliott R J 1987 *Phys. Rev. Lett.* **59**(20) 2337–2340
- [23] Wang H, Jiang M and Steel D G 1990 *Phys. Rev. Lett.* **65**(10) 1255–1258
- [24] Lambe J and Jaklevic R C 1968 *Phys. Rev.* **165**(3) 821–832
- [25] Klein J, Leger A, Belin M and Defourneau D 1973 *Phys. Rev. B* **7**(6) 2336–2348
- [26] Simonsen M G, Coleman R V and Hansma P K 1974 *J. Chem. Phys.* **61**(9) 3789–3799
- [27] Kirtley J R and Hansma P K 1975 *Phys. Rev. B* **12**(2) 531–536
- [28] Kirtley J R, Scalapino D J and Hansma P K 1976 *Phys. Rev. B* **14**(8) 3177–3184
- [29] Kirtley J R and Hansma P K 1976 *Phys. Rev. B* **13**(7) 2910–2917
- [30] Kirtley J R and Soven P 1979 *Phys. Rev. B* **19**(4) 1812–1817
- [31] Kirtley J R and Hall J T 1980 *Phys. Rev. B* **22**(2) 848–856
- [32] Persson B N J and Baratoff A 1987 *Phys. Rev. Lett.* **59**(3) 339–342
- [33] Agrait N, Untiedt C, Rubio-Bollinger G and Vieira S 2002 *Chem. Phys.* **281**(2) 231–234
- [34] Agrait N, Untiedt C, Rubio-Bollinger G and Vieira S 2002 *Phys. Rev. Lett.* **88**(21) 216803
- [35] Smit R H M, Noat Y, Untiedt C, Lang N D, van Hemert M C and van Ruitenbeek J M 2002 *Nature* **419** 906–909
- [36] Gregory S 1990 *Phys. Rev. Lett.* **64**(6) 689–692
- [37] Stipe B C, Rezaei M A and Ho W 1998 *Science* **280** 1732–1735
- [38] Stipe B C, Rezaei M A and Ho W 1998 *Phys. Rev. Lett.* **81**(6) 1263–1266
- [39] Stipe B C, Rezaei M A and Ho W 1999 *Phys. Rev. Lett.* **82**(8) 1724–1727
- [40] Hahn J R, Lee H J and Ho W 2000 *Phys. Rev. Lett.* **85**(9) 1914–1917
- [41] N Lorente N and Persson M 2000 *Phys. Rev. Lett.* **85**(14) 2997–3000
- [42] Galperin M, Ratner M A and Nitzan A 2004 *Nano Letters* **4**(9) 1605–1611
- [43] Williams J S 1998 *Materials Science and Engineering A* **253** 8–15
- [44] Cook I, Ward D and Dudarev S 2002 *Plasma Phys. Control. Fusion* **44** B121–B136
- [45] Bacon D J and Osetsky Y N 2002 *International Materials Reviews* **47**(5) 233–241
- [46] Huttner B 1998 *J. Phys.: Condens. Matter* **10** 6121–6126
- [47] Raimondi R, Savona G, Schwab P and Luck T 2004 *Phys. Rev. B* **70**(15) 155109
- [48] Usman E Y, Matulevich Y T and Urazgildin I F 2000 *Vacuum* **56** 293–297
- [49] Finnis M, Agnew P and Foreman J E 1991 *Phys. Rev. B* **44**(2) 567–574
- [50] Fu C C, dalla Torre J, Willaime F, Bocquet J L and Barbu A 2005 *Nature Materials* **4** 69–74
- [51] Horsfield A P, Bowler D R, Fisher A J, Todorov T N and Montgomery M J 2004 *J. Phys.: Condens. Matter* **16**(1) 3609–3622
- [52] Leggett A J, Chakravarty S, Dorsey A T, Fisher M P A, Garg A and Zwerger W 1987 *Rev. Mod. Phys.* **59**(1) 1–85
- [53] Henry C H and Lang D V 1977 *Phys. Rev. B* **15**(2) 989–1016
- [54] Tully J C 1977 *Phys. Rev. B* **16**(10) 4324–4334
- [55] Zener C 1932 *Proc. Royal Soc. A* **137**(833) 696–702
- [56] Landau L D 1932 *Phys. Z. USSR* **1** 88
- [57] Zhu C and Nakamura H 1994 *J. Chem. Phys.* **101**(12) 10630–10647
- [58] Kyanuma Y and Nakayama H 1998 *Phys. Rev. B* **57**(20) 13099–13112
- [59] Ridley B K 1999 *Quantum processes in semiconductors* (Clarendon Press)
- [60] Stoneham A M 1990 *Review of Solid State Science* **4**(2 & 3) 161–190
- [61] Persson B N J and Persson M 1980 *Solid State Commun.* **36**(2) 175–179
- [62] Montgomery M J, Todorov T N and Sutton A P 2002 *J. Phys.: Condens. Matter* **14**(1) 5377–5389
- [63] Montgomery M J, Hoekstra J, Todorov T N and Sutton A P 2003 *J. Phys.: Condens. Matter*

15(1) 731–742

[64] Montgomery M J and Todorov T N 2003 *J. Phys.: Condens. Matter* **15**(24) 8781–8795

[65] Chen Y C, Zwolak M and Di Ventra M 2003 *Nano Letters* **3** 1691

[66] Chen Y C, Zwolak M and Di Ventra M 2004 *Nano Letters* **4** 1709

[67] Chen Y C, Zwolak M and Di Ventra M 2005 *Nano Letters* **5** 621

[68] Yang Z, Chshiev M, Zwolak M, Chen Y C and Di Ventra M 2005 *Phys. Rev. B* **71** 041402

[69] Zhitenev N B, Meng H and Bao Z 2002 *Phys. Rev. Lett.* **88** 226801

[70] Persson B N J and Demuth J E 1984 *Phys. Rev. B* **30**(10) 5968–5986

[71] Persson B N J and Demuth J E 1986 *Solid State Commun.* **57**(9) 769–772

[72] Caroli C, Combescot R, Nozieres P and Saint-James D 1971 *J. Phys. C* **4**(8) 916–929

[73] Caroli C, Combescot R, Lederer D, Nozieres P and Saint-James D 1971 *J. Phys. C* **4**(16) 2598–2610

[74] Combescot R 1971 *J. Phys. C* **4**(16) 2611–2622

[75] Caroli C, Combescot R, Nozieres P and Saint-James D 1972 *J. Phys. C* **5**(1) 21–42

[76] Martin-Rodero A, Flores F and March N H 1988 *Phys. Rev. B* **38**(14) 10047–10050

[77] Ferrer J, Martin-Rodero A and Flores F 1988 *Phys. Rev. B* **38**(14) 10113–10115

[78] Meir Y and Wingreen N S 1992 *Phys. Rev. Lett.* **68** 2512

[79] Brandbyge M, Mozos J L, Ordejon P, Taylor J and Stokbro K 2002 *Phys. Rev. B* **65**(16) 165401

[80] Todorov T N 2002 *J. Phys.: Condens. Matter* **14**(1) 3049–3084

[81] Doyen G 1993 *J. Phys.: Condens. Matter* **5** 3305

[82] Ness H and Fisher A J 1997 *Phys. Rev. B* **56** 12469

[83] Bruus H and Flensberg K 2004 *Many-body Quantum Theory in Condensed Matter* (Oxford: Oxford University Press)

[84] Keldysh L 1965 *Sov. Phys. JETP* **20** 1018

[85] Kadanoff L P and Baym G 1962 *Quantum Statistical Mechanics* (New York: W.A. Benjamin)

[86] Sols F 1992 *Annals of Physics* **214** 386

[87] Bonča J and Trugman S 1995 *Phys. Rev. Lett.* **75** 2566

[88] Ness H and Fisher A J 1999 *Phys. Rev. Lett.* **83** 452

[89] Haule K and Bonča J 1999 *Phys. Rev. B* **59** 13087

[90] Mingo N and Makoshi K 2000 *Phys. Rev. Lett.* **84** 3694

[91] Ness H, Shevlin S A and Fisher A J 2001 *Phys. Rev. B* **63** 125422

[92] Ness H and Fisher A J 2002 *Europhys. Lett.* **57** 885

[93] Ness H and Fisher A J 2002 *Chem. Phys.* **281** 279

[94] Troisi A, Ratner M A and Nitzan A 2003 *J. Chem. Phys.* **118** 6072

[95] Troisi A and Ratner M A 2005 *Phys. Rev. B* **72** 033408

[96] Jiang J, Kula M, Lu W and Luo Y 2005 *Nano Letters* **5** 1551

[97] Bihary Z and Ratner M A 2005 *Phys. Rev. B* **72**(11) 115439

[98] Ness H and Fisher A J 2005 *Proc. Nat. Acad. Sci. USA* **102** 8826

[99] Mahan G D 1990 *Many-Particle Physics* (New York: Plenum Press)

[100] Rammer J and Smith H 1986 *Rev. Mod. Phys.* **58** 323

[101] Inglesfield J 1981 *J. Phys. C: Sol. State Phys.* **14** 3795

[102] Datta S 1995 *Electronic Transport in Mesoscopic Systems* (Cambridge: Cambridge University Press)

[103] Frederiksen T, Brandbyge M, Lorente N and Jauho A 2004 *Phys. Rev. Lett.* **93** 256601

[104] Paulsson M, Frederiksen T and Brandbyge M 2005 *Phys. Rev. B* **72** 201101

[105] Hyldgaard P, Hershfield S, Davies J H and Wilkins J W 1994 *Annals of Physics* **236** 1

[106] Mii T, Tikhodeev S and Ueba H 2002 *Surface Science* **502**–**503** 26

[107] Mii T, Tikhodeev S and Ueba H 2003 *Phys. Rev. B* **68** 205406

[108] Galperin M, Ratner M A and Nitzan A 2004 *J. Chem. Phys.* **121** 11965

[109] Mitra A, Aleiner I and Millis A J 2004 *Phys. Rev. B* **69** 245302

[110] Ryndyk D A, Hartung M and Cuniberti G 2005 (*Preprint cond-mat/0508143*)

[111] Peccia A, Di Carlo A, Gagliardi A, Sanna S, Frauenheim T and Gutierrez R 2004 *Nano Letters* **4** 2109

[112] Peccia A and Di Carlo A 2004 *Rep. Prog. Phys.* **67** 1497

[113] Asai Y 2004 *Phys. Rev. Lett.* **93** 246102

[114] Asai Y 2004 *Phys. Rev. Lett.* **94** 099901(E)

[115] Viljas J K, Cuevas J C, Pauly F and Häfner M 2005 *Phys. Rev. B* **72** 245415

[116] de la Vega L, Martin-Rodero A, Agraït N and Yeyati A L 2005 (*Preprint cond-mat/0511287*)

[117] Mahan G 1987 *Physics Report* **145** 251

[118] Rammer J 1991 *Rev. Mod. Phys.* **63** 781

[119] Jacoboni C and Bordone P 2004 *Rep. Prog. Phys.* **67** 1033–1071

- [120] Horsfield A P, Bowler D R, Fisher A J, Todorov T N and Sanchez C G 2004 *J. Phys.: Condens. Matter* **16**(46) 8251–8266
- [121] Horsfield A P, Bowler D R, Fisher A J, Todorov T N and Sanchez C G 2005 *J. Phys.: Condens. Matter* **17** 4793–4812
- [122] Todorov T N, Sanchez C G, Bowler D R and Horsfield A P 2005 Ψ_K *Newsletter* **68** 69–91
- [123] Bowler D R, Horsfield A P, Sanchez G S and Todorov T N 2005 *J. Phys.: Condens. Matter* **17** 3985–3995
- [124] Theilhaber J 1992 *Phys. Rev. B* **46**(20) 12990–13003
- [125] Parandekar P and Tully J 2005 *J. Chem. Phys.* **122**(9) 094102
- [126] Hack M and Truhlar D 2000 *J. Phys. Chem. A* **104**(34) 7917–7926
- [127] Hack M and Truhlar D 2001 *J. Chem. Phys.* **114**(21) 9305–9314
- [128] Zhu C, Jasper A and Truhlar D 2004 *J. Chem. Phys.* **120**(12) 5543–5557
- [129] CY Z, S N, Jasper A and Truhlar D 2004 *J. Chem. Phys.* **121**(16) 7658–7670
- [130] Diestler D J 1983 *J. Chem. Phys.* **78**(5) 2240–2247
- [131] Kilin D S, Pereversev Y V and Prezhdo O V 2004 *J. Chem. Phys.* **120**(23) 11209–11223
- [132] Baer R and Siam N 2004 *J. Chem. Phys.* **121**(13) 6341–6345
- [133] Johansson A and Stafstrom S 2004 *Phys. Rev. B* **69**(23) 235205
- [134] An Z, Wu C and Sun X 2004 *Phys. Rev. Lett.* **93**(21) 216407
- [135] Block S and Streitwolf H 1996 *J. Phys.: Condens. Matter* **8**(7) 889–900
- [136] Tully J C and Preston R K 1971 *J. Chem. Phys.* **55** 562–572
- [137] Tully J C 1990 *J. Chem. Phys.* **93** 1061–1071
- [138] Hammesschiffer S and Tully J C 1994 *J. Chem. Phys.* **101** 4657–4667
- [139] Todorov T N 2001 *J. Phys.: Condens. Matter* **13**(1) 10125–10148
- [140] Fang J Y and Hammes-Schiffer S 1999 *J. Phys. Chem. A* **103** 9399–9407
- [141] Topaler M, Hack M, Allison T, Liu Y P, Mielke S, Schwenke D and Truhlar D 1997 *J. Chem. Phys.* **106**(21) 8699–8709
- [142] Topaler M S, Allison T C, Schwenke D W and Truhlar D G 1998 *J. Chem. Phys.* **109** 3321–3345
- [143] Tully J C 1998 *Faraday Discussions* pp 407–419
- [144] Bach C and Gross A 2001 *J. Chem. Phys.* **114** 6396–6403
- [145] Coker D F and Xiao L 1995 *J. Chem. Phys.* **102** 496–510
- [146] Herman M F 1995 *J. Chem. Phys.* **103** 8081–8097
- [147] Sholl D S and Tully J C 1998 *J. Chem. Phys.* **109** 7702–7710
- [148] Blais N C and Truhlar D G 1983 *J. Chem. Phys.* **79** 1334–1342
- [149] Volobuev Y L, Hack M D, Topaler M S and Truhlar D G 2000 *J. Chem. Phys.* **112** 9716–9726
- [150] Prezhdo O V and Rossky P J 1997 *J. Chem. Phys.* **107** 825–834
- [151] Space B and Coker D F 1991 *J. Chem. Phys.* **94** 1976–1984
- [152] Prezhdo O V and Rossky P J 1996 *J. Phys. Chem.* **100** 17094–17102
- [153] Drukker K and de Leeuw S W 1998 *Chem. Phys. Lett.* **291** 283–290
- [154] Wong K F and Rossky P J 2001 *J. Phys. Chem. A* **105** 2546–2556
- [155] Batista V S and Coker D F 1996 *J. Chem. Phys.* **105** 4033–4054
- [156] Batista V S and Coker D F 1997 *J. Chem. Phys.* **106** 6923–6941
- [157] Niv M Y, Krylov A I, Gerber R B and Buck U 1999 *J. Chem. Phys.* **110** 11047–11053
- [158] Niv M Y, Bargheer M and Gerber R B 2000 *J. Chem. Phys.* **113** 6660–6672
- [159] Alberti S F, Echave J, Engel V, Halberstadt N and Beswick J A 2000 *J. Chem. Phys.* **113** 1027–1034
- [160] Winter N, Chorny I, Vieceli J and Benjamin I 2003 *J. Chem. Phys.* **119** 2127–2143
- [161] Winter N and Benjamin I 2004 *J. Chem. Phys.* **121** 2253–2263
- [162] Cattaneo P and Persico M 1998 *Chem. Phys. Lett.* **289** 160–166
- [163] Cattaneo P, Granucci G and Persico M 1999 *J. Phys. Chem. A* **103** 3364–3371
- [164] Cattaneo P and Persico M 2001 *J. Am. Chem. Soc.* **123** 7638–7645
- [165] Lobaugh J and Rossky P J 1999 *J. Phys. Chem. A* **103** 9432–9447
- [166] Ito M and Ohmine I 1997 *J. Chem. Phys.* **106** 3159–3173
- [167] Groenhof G, Bouxin-Cademartory M, Hess B, Visser S P D, Berendsen H J C, Olivucci M, Mark A E and Robb M A 2004 *J. Am. Chem. Soc.* **126** 4228–4233
- [168] Warshel A and Chu Z T 2001 *J. Phys. Chem. B* **105** 9857–9871
- [169] Ciminelli C, Granucci G and Persico M 2004 *Chemistry-a European J.* **10** 2327–2341
- [170] Yokozawa A and Miyamoto Y 2000 *J. Appl. Phys.* **88** 4542–4546
- [171] Bruening J and Friedman B 1997 *J. Chem. Phys.* **106** 9634–9638
- [172] Frank I, Hutter J, Marx D and Parrinello M 1998 *J. Chem. Phys.* **108** 4060–4069
- [173] Doltsinis N L and Marx D 2002 *Phys. Rev. Lett.* **88**
- [174] Doltsinis N L 2004 *Mol. Phys.* **102** 499–506

[175] Langer H and Doltsinis N L 2004 *Phys. Chem. Chem. Phys.* **6** 2742–2748

[176] Craig C F, Duncan W R and Prezhdo O V 2005 *Phys. Rev. Lett.* **95**

[177] Herman M F 2005 *J. Phys. Chem. A* **109** 9196–9205

[178] Thorndyke B and Micha D A 2005 *Chem. Phys. Lett.* **403** 280–286

[179] Nielsen S, Kapral R and Ciccotti G 2000 *J. Phys. Chem.* **112**(15) 6543–6553

[180] Baranger M, de Aguiar M A M, Keck F, Korsch H J and Schellhaass B 2001 *J. Phys. A: Math. Gen.* **34** 7227–7286

[181] Miller W H 2001 *J. Phys. Chem. A* **105** 2942–2955

[182] Herman M F 1994 *Annu. Rev. Phys. Chem.* **45** 83–111

[183] Makri N 1999 *Ann. Rev. Phys. Chem.* **50** 167–191

[184] Heller E J 1975 *J. Chem. Phys.* **62** 1544–1555

[185] Heller E J 1975 *J. Chem. Phys.* **64** 63–73

[186] Heller E J 1976 *J. Chem. Phys.* **65** 4979–4989

[187] Heller E J 1977 *J. Chem. Phys.* **66** 5777–5785

[188] Heller E J 1977 *J. Chem. Phys.* **67** 3339–3351

[189] Davis M J and Heller E J 1979 *J. Chem. Phys.* **71** 3383–3395

[190] Heller E 1981 *J. Chem. Phys.* **75** 2923–2932

[191] van Vleck J H 1928 *Proc. Natl. Acad. Sci. USA* **14** 178

[192] Sun X and Miller W H 1997 *J. Chem. Phys.* **106** 916–927

[193] Pechukas P 1969 *Phys. Rev.* **181** 166

[194] Herman M F and Kluk E 1984 *Chem. Phys.* **91** 27

[195] Kluk E, Herman M F and Davis H L 1985 *J. Chem. Phys.* **84**(1) 326–334

[196] Herman M F 1986 *J. Chem. Phys.* **85** 2069–2076

[197] Walton A R and Manolopoulos D E 1996 *Mol. Phys.* **87** 961–978

[198] Heller E J 1991 *J. Chem. Phys.* **94** 2723–2729

[199] Elran Y and Kay K G 1999 *J. Chem. Phys.* **110** 3653–3659

[200] McCormack D A 1999 *J. Chem. Phys.* **112** 992–1001

[201] Schwartz B J, Bittner E R, Prezhdo O and Rossky P J 1996 *J. Chem. Phys.* **104** 5942–5955

[202] Neria E and Nitzan A 1993 *J. Chem. Phys.* **99** 1109–1123

[203] Herman M F and Coker D F 1999 *J. Chem. Phys.* **111** 1801–1808

[204] Noid W G, Ezra G S and Loring R F 2003 *J. Chem. Phys.* **119** 1003–1020

[205] Brewer M L 1999 *J. Chem. Phys.* **111** 6168–6170

[206] Sun X, Wang H and Miller W H 1998 *J. Chem. Phys.* **109** 7064–7074

[207] Miller W H 1970 *J. Chem. Phys.* **53** 1949–1959

[208] Wang H, Song X, Chandler D and Miller W H 1999 *J. Chem. Phys.* **110** 4828–4840

[209] Martinez T J, Ben-Nun M and Levine R D 1996 *J. Phys. Chem.* **100** 7884–7895

[210] Martinez T J, Ben-Nun M and Levine R D 1997 *J. Phys. Chem. A* **101** 6389–6402

[211] Ben-Nun M and Martinez T J 1998 *J. Chem. Phys.* **108** 7244–7257

[212] Martinez T J 2005 *Acc. Chem. Res.* **in press**

[213] Zhu C, Nobusada K and Nakamura H 2001 *J. Chem. Phys.* **115** 3031–3044

[214] Zhu C, Kamisaka H and Nakamura H 2001 *J. Chem. Phys.* **115** 11036–11039

[215] Kondorskiy A and Nakamura H 2004 *J. Chem. Phys.* **120** 8937–8954

[216] Hillery M, O'Connell R F, Scully M O and Wigner E P 1984 *Physics Reports* **106**(3) 121–167

[217] Billing G D 1999 *J. Chem. Phys.* **110**(12) 5526–5537

[218] Prezhdo O V and Pereverzev Y V 2000 *J. Chem. Phys.* **113**(16) 6557–6565

[219] Horsfield A, Bowler D and Fisher A 2004 *J. Phys.: Condens. Matter* **16**(7) L65–L72

[220] Burt M G 1982 *J. Phys. C: Solid State Phys.* **15** L381–L384

[221] Wigner E 1932 *Phys. Rev.* **40** 749–759

[222] Kapral R and Ciccotti G 1999 *J. Chem. Phys.* **110**(18) 8919–8929

[223] Abrikosov A A, Gorkov L P and Dzyaloshinski I E 1963 *Methods of Quantum Field Theory in Statistical Physics* (New York: Dover)

[224] Fetter A L and Walecka J D 1971 *Quantum Theory of Many-Particle Systems* (New York: McGraw-Hill)

[225] Galperin M, Nitzan A and Ratner M A 2005 (*Preprint cond-mat/0510452*)

[226] Haug H and Jauho A 1996 *Quantum Kinetics in Transport and Optics of Semi-conductors* (Berlin: Springer-Verlag)

[227] Jauho A P 2005 (*Preprint cond-mat/0510229*)